Application of a "Radiation-type" Boundary Condition To the Wave-porous Problem

C.R. McClain, N.E. Huang, L.J. Pietrafesa
May 1977

APPLICATION OF A RADIATION-TYPE BOUNDARY CONDITION TO
TO THE WAVE-POROUS BED PROBLEM

by

Charles R. McClain
Norden E. Huang
Leonard J. Pietrafesa

Department of Geosciences and Center for Marine and Coastal Studies
North Carolina State University

ACKNOWLEDGMENTS

ABSTRACT·

Many coastal states, and in particular North Carolina, have had to address the problem of the effects of coastal sediments having been transported, usually under severe oceanic and atmospheric storm conditions. Typically, the states address such problems only after (or during) a catastrophe has (or is) occurred (occurring). This is an attempt at delving into one small aspect of the overall study of understanding the physics governing the transport of coastal sediments and of the interactive effects between the oceanic fluid and sediment media.

The problem of a small-amplitude wave propagating over a flat porous bed is reanalyzed subject to the bottom boundary condition,

$$\frac{\partial u}{\partial z}\Big|_o = \frac{\alpha}{\sqrt{K}} \left(u\big|_o - \tilde{u}_s\big|_o\right)$$

where u represents the horizontal velocity in the fluid, $\tilde{u}_s$ represents the horizontal velocity within the bed as predicted by Darcy's law, K is the permeability and the subscript "o" denotes evaluation at the bottom, $z = 0$. The term, α, is a constant whose value depends on the porosity of the bed at the interface and must be determined experimentally. The boundary condition is of the form of a "radiation-type" condition commonly encountered in heat conduction problems.

The important physical quantities (velocity, velocity potential, stream functions, shear stress and energy dissipation) have been derived and are presented, subject to natural conditions. The bottom boundary layer is represented by the linearized Navier-Stokes equations under the usual boundary layer approximations. It is found that the boundary layer velocity distribution and shear stress can be greatly altered from impermeable bed predictions. Theoretical results for energy dissipation and shear stress are compared to existing data and are found to agree very well. The predictions of classical small amplitude wave theory are not appreciably modified away from the boundary.

TABLE OF CONTENTS

v

LIST OF TABLES

LIST OF FIGURES

1 INTRODUCTION

1.1 Purpose

As ocean waves propagate away from their generation areas, they eventually encounter the coastal zone and, subsequently, sediments which constitute a loose bottom boundary to the wave motion. Seaward of the coastal zone, modifications of the propagating waves have been due to interactions with other surface waves, surface currents, internal waves, viscous and turbulent energy dissipation, and continued interaction with the atmosphere. Since the water is initially "deep," i.e., depth/wavelength > 1/2, the wave group is dispersive (meaning the phase speed depends on the wave length). The longest waves, called forerunners, encounter the "shallow" water $(\frac{d}{L} < \frac{1}{20})$ first because they travel faster and induce deeper fluid motions. Komar et al. (1972) have photographed deep-water oscillatory ripple marks off the Oregon coast at depths of 200 meters. It is therefore quite possible for a wave to have considerable interplay with the bottom before reaching the beach. This is especially true along wide continental shelves. From this point of view, the wave-bottom interaction becomes of great practical importance to the activities of man. The design of coastal structures and port facilities as well as the management of navigable waterways are functions of predicted wave parameters and sediment transport.

The study of waves propagating over a porous, erodible bed has only in recent years received more than passing attention by the scientific community (see Figure 1.1). Meanwhile, the associated phenomenon of uniform flow over loose boundaries has received serious attention for over

2

n

MWL

Wave Potential Field

d

Viscous Boundary

Layers

h

Porous Bed
(Darcy's law)

Impermeable Layer
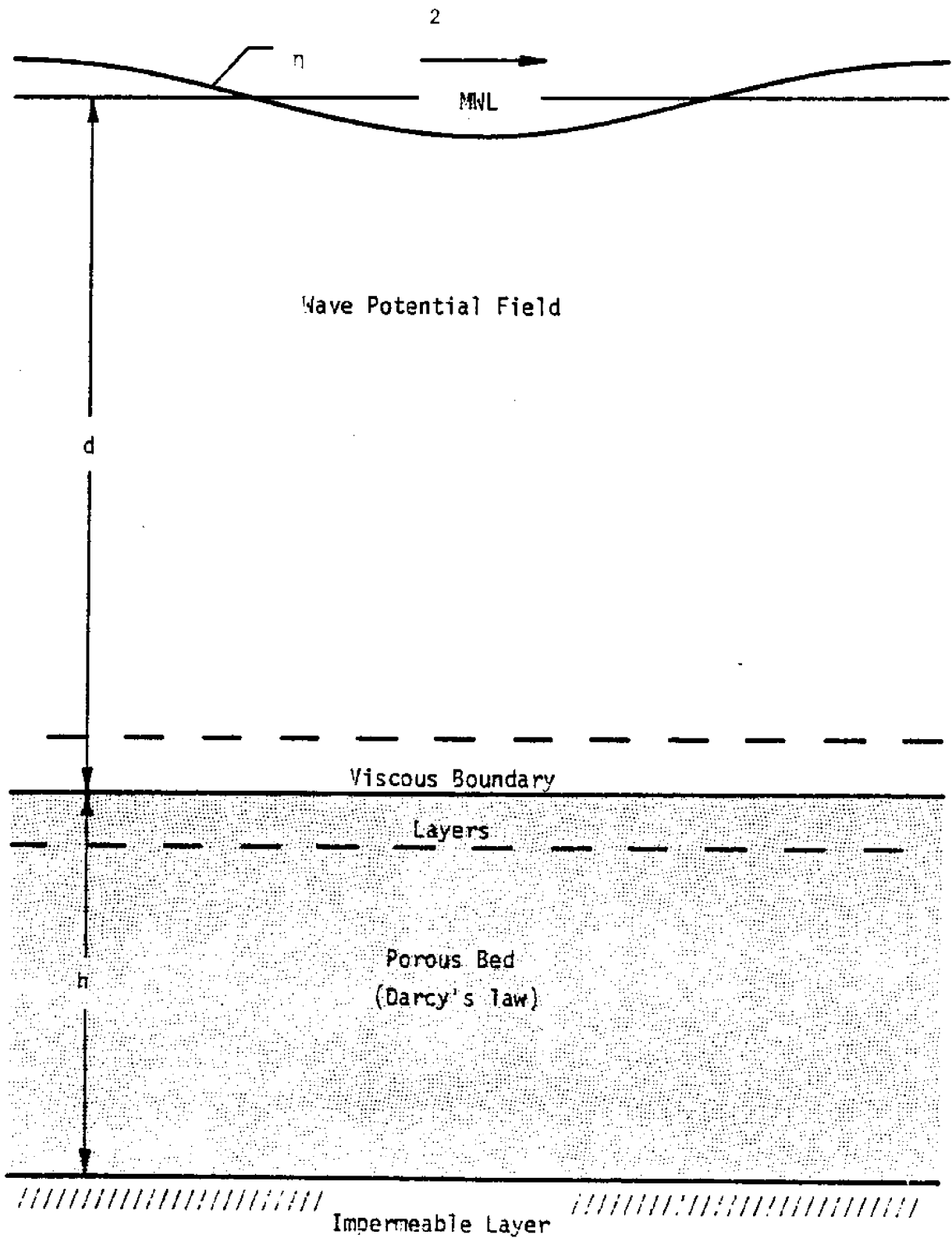
Figure 1.1   Flow fields

two centuries, although description of either the flow field or the bed configuration, whether analytic or descriptive, remains incomplete (Jain and Kennedy, 1974; McQuivey, 1973), as does determination of the resulting sediment transport (Yalin, 1972). No doubt the physics of the wave associated problem is becoming better understood due to recent technological advances in instrumentation and data analysis, but until a better understanding of turbulence and sediment mechanics is obtained, predictive capability will remain only qualitative. The key to a more complete understanding will be in the thorough knowledge of the boundary layer flow since all of the important parameters (flow fields, shear stress distribution, boundary layer velocity profile and energy dissipation) are functionally dependent on the dynamic character of this layer.

The purpose of this work is to investigate porous bed effects and their relative importance upon an Airy wave in "intermediate" ($.05 < d/L < .5$) and "shallow" water depths. Particular attention is directed towards the bottom boundary condition to be used, because it will have significant effects on the wave and bed flow properties, especially in the boundary layer. A large number of assumptions are made which limit practical application to a certain extent, but judicious deletion of particular terms in the equations of motion allow analytic solution of the coupled problem and clarifies the influence of the boundary condition.

It is appropriate to dicuss the assumptions as listed in Table 1.1 and to present results of other investigations which shed light on the credence of the approximations. The following sections will serve this purpose, along with an introduction to the wave theory which will be used.

Table 1.1 List of assumptions

A. On the nature of the fluid

    1. Incompressible

    2. Small viscosity

    3. Homogeneous

B. Nature of the environment

    1. No atmospheric interaction

    2. No currents

    3. Irrotational motion above boundary layer

    4. Nonsloping bottom

    5. Smooth interface

C. Wave theory selection

    1. Airy or Small Amplitude Wave Theory

D. Nature of the bottom flow regime and boundary
    layer equations

    1. Laminar

    2. Linearized

E. Nature of the porous bed and flow

    1. Statistically homogeneous

    2. Darcy's law applicable

1.2 Nature of the Fluid

The problem includes, in effect, a multi-phase fluid. The principle component under consideration is sea water. Of the assumptions made, those concerning the sea water phase are the most exact. It is common practice to regard it as incompressible, although it is compressible to a small extent. It has been estimated that if water were truly incompressible, the sea would rise by more than 30 meters. The mean compressibility is a function of the temperature, salinity and in situ pressure, but its value lies in the neighborhood of $4.3 \times 10^{-5} \ m^2$ /Newton for the surface layer. This places the speed of sound in the vicinity of 1.5×10^3 m/sec and therefore the Mach number is bound to be very small. Thus, as far as particle dynamics are concerned the fluid is incompressible, i.e., the volume of a control volume is assumed pressure independent (Lighthill, 1963).

Water can be considered inviscid except near a boundary. Since we are not considering situations where high concentrations of suspended sediment exist, such as in turbidity currents, the fluid is assumed Newtonian and has a molecular viscosity of the order of 10^{-2} gr/cm·sec. As will be shown in the discussion of the laminar boundary layer, viscous effects are limited to a region only a few centimeters in thickness.

The density of sea water rarely fluctuates by more than 5 percent of its mean value with a few notable exceptions, such as the Red Sea, where hypersaline layers exist. Strong thermoclines are characteristic of the Red Sea and can occur within the depth range of surface influence. Generally, density variations can be important in studying large-scale

thermohaline circulation and internal wave phenomena, but herein the effects of variability in the density field will be neglected.

1.3 Nature of the Environment

Air-sea interaction will not be considered in this development. Additionally, even though it is known that surface tension is important to momentum transport across the surface interface via capillary and capillary-gravity waves, it will be assumed that waves of these order wave lengths are of no significance to bottom interactions.

On the other hand, currents can be significant near the bottom. Strong currents are commonly encountered in the near-shore zone and along the continental shelf and slope. Tidal inlets and estuary mouths can greatly modify incoming waves in localized areas (Boone, 1974). Usually variable depths should be considered in these locations since large ebb deltas can be present. Waves can also induce nearshore currents called rip currents and longshore currents. Western boundary currents, such as the Gulf Stream, can produce considerable modification of the wave field. These currents usually appear seaward of the shelf break, but "spin-off" eddies and "shingles" occasionally occur and advect across the shelf resulting in considerable mixing and nutrient influx. However, eddies are secondary sources of currents compared to wind-driven circulation which is generally present and can, during storms, be considerable, i.e., 1 m/sec, in magnitude. Under such conditions, the surface displacement will be more random than monochromatic, with considerable breaking of the waves being present. Although the sea state is important, our primary objective is to understand the boundary layer. Therefore, using one component will be

sufficient. The result can be generalized to complicated combinations of wave components without additional difficulty in principle. Also, since conditions on the shelf which would initiate significant currents with respect to the wave motion result in several poorly understood phenomena, currents on the shelf will not be considered and the theory developed herein will simply not be valid near strong nearshore currents.

The next assumption, that of nonsloping bottom, is reasonably true since the average shelf slope is of the order of 0.1° . Of course, rapid depth changes do occur in the vicinity of shoals, nearshore bars, and the beach. These are usually connected with wave breaking and are rather localized topographical features and therefore will not be considered. Radwan et al. (1975) have obtained semi-closed form solutions for small-amplitude waves in currents over slowly varying bottom depths. Boundary layer considerations were not included in their work.

In conclusion, although the author recognizes that the atmosphere, depth and currents can have important effects, to consider them would lead this investigation astray from its specified purpose. Discussion of irrotationality will be included in section 1.4 and the smooth and stationary interface assumptions will be included in section 1.5.

1.4 Wave Theory

Under the assumptions of section 1.2 and considerations of section 1.3, the equations governing the flow in the main body of fluid reduce to the two-dimensional Bernoulli and continuity equations and a statement of irrotationality. According to Kelvin's circulation theorem, irrotationality can be assumed if the wave propagates into an initially irrotational volume of fluid.

$$\underline{u}_t + (\underline{u} \cdot \underline{\nabla}) \, \underline{u} + \underline{\nabla} \, p/\rho + g\underline{z} = 0 \qquad\qquad (1.1)$$

$$\underline{\nabla} \cdot \underline{u} = 0 \, , \qquad \underline{\nabla} \times \underline{u} = 0 \qquad\qquad (1.2, \ 1.3)$$

where $\underline{u} = (U, W)$, $\underline{\nabla} = (\partial/\partial x, \partial/\partial z)$ and underscored quantities are vectors. The appropriate boundary conditions at the surface, $z = \eta + d$, d being the mean water depth,

are $\qquad \eta_t + U \cdot \eta_x = W$ (kinematic) $\qquad$ (1.4)

and $\qquad \phi_t + \frac{1}{2} (\phi_x^2 + \phi_z^2) + gz = 0$ (dynamic) $\qquad$ (1.5)

where $U = \phi_x$ and $W = \phi_z$. At the bottom, $z = 0$, the impermeable condition is

$$W_0 = 0 \, . \qquad\qquad (1.6)$$

Of course, this condition will be altered in this paper, but it is assumed in the theories discussed below. The exact solution of these equations has been obtained only in special cases and an approximation method must be employed in other cases.

There are over a dozen wave theories in existence (see LeMehauté, et al., 1968). Each has a limited range of application for values of a/d, a/L, and d/L (see Figure 1.2), where a, d, and L are the amplitude, depth, and wavelength, respectively. The large number of theories stem from the approximations made regarding the relative sizes of these three parameters and the manner in which the solution is derived. The solution is obtained in one of two ways as decribed by Dean and Eagleson (1966). The first is a perturbation of the solution (Stokes
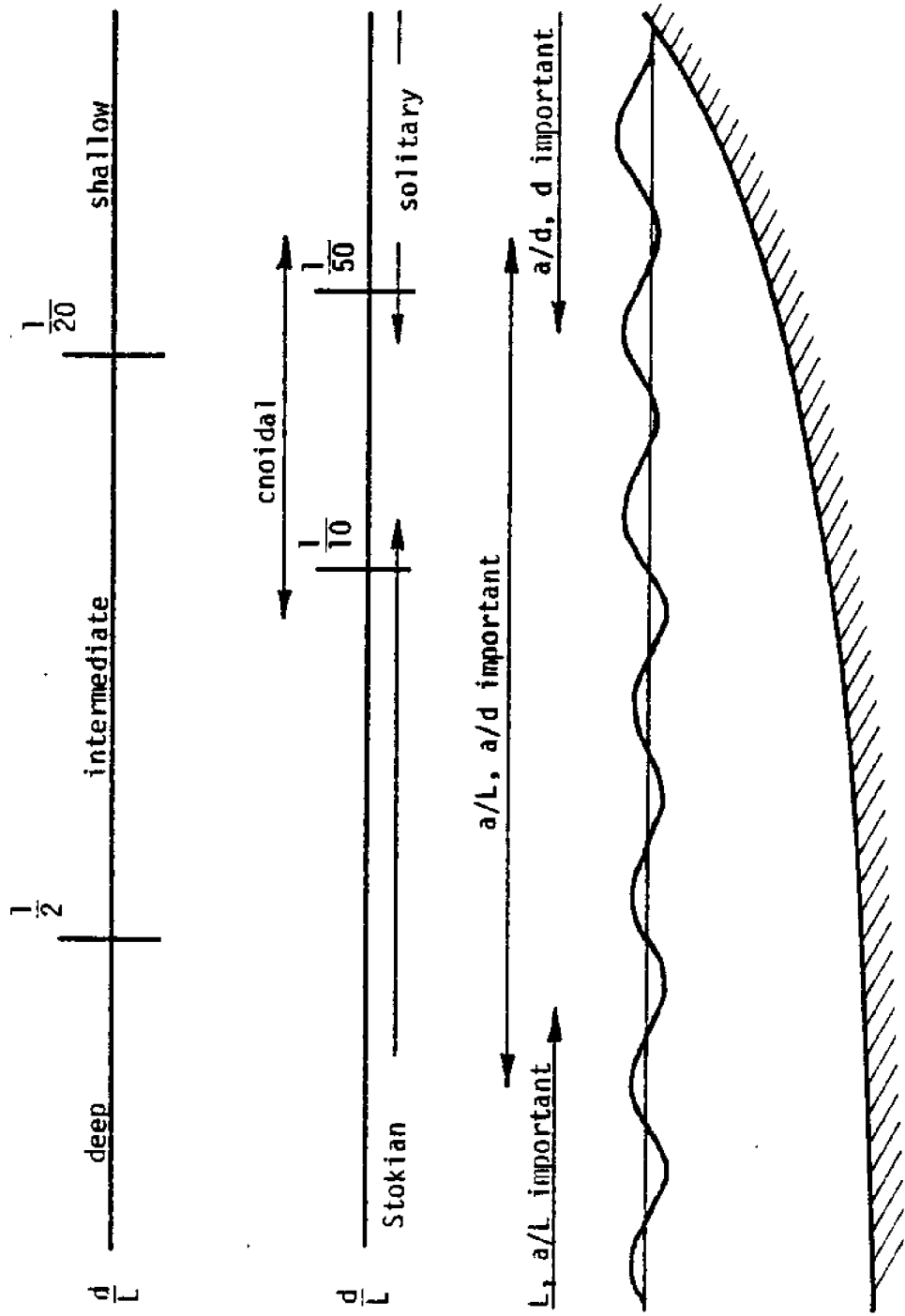
Figure 1.2 Classification of wave theories (Dean and Eagleson, 1966)

waves), and the second is a perturbation of both the solution and the governing equations (cnoidal waves). Solitary waves are occasionally thought of as being in a separate class, but Peregrine (1972) points out that they are cnoidal waves of infinite wavelength.

The perturbation scheme is employed using one of the above ratios as the expansion parameter and the result will be valid for various ranges of the other two. The ranges of validity of such solutions have been investigated by Keulegan (1950) and Laitone (1962), but the exact limits of validity are not well established. The most generally used theory is Stokian mainly because of its ease of application, especially the first-order solution (commonly called Airy, or small-amplitude wave theory). Higher-order Stokes and cnoidal results can be obtained from tables (Skjelbreia, 1959; Masch, 1961), and LeMehaute et al. (1968) compared twelve wave theories and found the cnoidal theory of Keulegan and Patterson (1940) to perform the best under conditions usually encountered in site-specific engineering problems.

First-order Stokian theory is valid for all values of d/L since it assumes both a/L and a/d to be small while higher-order Stokes theories are valid in deep water when a/L is finite (see Figure 1.2). Because of its uniform validity for all d/L and its simplicity, it is used in this paper.

1.5 Nature of the Bottom Flow Regime

Boundary roughness, bed mobility, and the flow regime at the bottom are all interdependent and are discussed together. The theory developed

herein assumes a smooth, stationary bed with a linearized boundary layer. The boundary condition for a mobile, saltating bed has not been developed and any theory developed so far is limited by the threshold conditions.

As mentioned previously, potential flow is used and therefore no boundary condition on U, the horizontal velocity component, can be satisfied at the bottom. Thus a slip condition exists, i.e., U assumes an unrealistic value at the bottom. All fluids are viscous and while viscous effects may not be important in the main body of our fluid, its effect near the interface is very important for a number of reasons. First, viscous forces near the interface are the most important source of energy dissipation in shallow water waves. Secondly, the tangential stress due to viscosity initiates sediment motion and, along with mass transport, causes sediment transport. The term mass transport should not be confused with sediment transport. Mass transport refers to the mean Lagrangian displacement of fluid particles over a wave period and is sometimes referred to as the wave entrainment current. Mass transport also results from inertial effects appearing in the second-order Stokian theory. The topic has been discussed by Lonquet-Higgins (1958) and more recently by Huang (1970) for a linearized laminar boundary layer. Sleath (1968) has noted that a porous bed enhances mass transport.

If the flow regime is taken to be laminar, the validity of assuming a linearized laminar boundary layer has been questioned by Grosch (1962), Iwagaki et al. (1967), and Teleki (1972). Grosch and Iwagaki et al., using different methods of solution, concluded that nonlinear effects in a laminar boundary layer in the presence of an Airy

wave have little effect on energy dissipation or on the magnitude of the bottom shear stress, $\tau_0 = \mu \partial^2 u / \partial z^2|_0$. However, Teleki found that inclusion of the nonlinear terms resulted in the phase lag between τ_0 and the external driving velocity decreasing from $\pi/4$ to $\pi/6$. The direct measurement of wave shear stresses has been undertaken by Eagleson (1962) and Iwagaki et al. (1965) for smooth bottoms using shear plates and torque gages with the latter group making considerable improvement in instrumentation.

The next question to arise concerns the conditions under which the boundary layer can be assumed to be laminar. This involves surface roughness as well as the Reynolds number. Experiments by Vincent (1957) and Collins (1963) indicate that wave tank boundary layers over smooth bottoms will almost always be laminar, whereas prototype shallow water waves will have turbulent boundary layers. This points out the well-known scaling problem of wave tanks. For this reason, Jonsson (1963) and Riedel et al. (1972) have used oscillating water tunnels for measuring velocity profiles and shear stresses, respectively, in oscillating flows under prototype conditions. The criterion developed by Collins is $U_0 \delta / \nu = 160$, which is nearly 1/4 that proposed by Li (1954) who used a smooth oscillating bottom. δ is the boundary layer thickness. Their methods of determining transition flow were quite different; Collins used measurements of mass transport and Li used dyes. However, Li's results were biased by the fact that the dyes were more dense than the surrounding fluid. Kalkanis (1957) reperformed the experiments on a smooth bottom using dyes of specific gravity 1.0 and showed that turbulence occurred at lower Reynolds numbers than found by Li, a result more consistent with those of Vincent and Col-

lins. Kalkanis also developed semi-empirical equations for the velocity profile.

When the bottom is rough, the critical Reynolds number will be lower. If the roughness length is a fractional value of the boundary layer thickness, the interface is called "hydrodynamically smooth;" if it is not, it is called "hydrodynamically rough." Criteria for these terms were considered in detail by Li (1954) and Manohar (1955), who obtained the same results which are shown below along with determinations for critical Reynolds numbers, as given by Einstein (1972). The data cited by Einstein included flow over rigid, artificial ripples for linear (two-dimensional) and irregular (three-dimensional) featured cases. (See Table 1.2).

The term "rough" also includes consideration of bed forms. Early studies on the initiation of sediment motion and bed form growth were conducted by Bagnold (1946), and by Manohar (1955), in oscillating tanks. The bed is always made smooth, i.e., void of bed forms, when studying thresholds of sediment motion. Bed forms are the result of such motions. Bagnold's results were used by Putnam and Johnson (1949) to estimate wave attenuation due to bottom friction. Savage (1953) performed wave tank experiments on energy losses due to bottom friction over smooth and rippled surfaces and also losses due to bed percolation. He found that energy was expended most rapidly while the bed was attaining its equilibrium configuration. Once the bed becomes unstable, the boundary condition becomes more complex and the boundary layer will be greatly affected. It is therefore rather important to understand when bed motion will begin.

Table 1.2 Criteria for roughness and flow regime

Smooth Boundary $\qquad$ $\delta/z_0 > 6.54$

Transition $\qquad$ $4.02 < \delta/z_0 < 6.54$

Rough Boundary $\qquad$ $\delta/z_0 < 4.02$

where z = roughness length and

δ = boundary layer thickness = $6.5\sqrt{\nu/\sigma}$

$Re_c = a^2\sigma/\nu = 1.7 \cdot 10^5$ $\qquad$ smooth boundary

$Re_c = z_0 a\sigma/\nu = 640$, 2-D roughness, $a/z_0 < 266$

" $= 104$, 3-D roughness, $a/z_0 < 1630$

where a = excursion amplitude of bottom plate and

Re_c = critical Reynold's number

Comment: Other definitions of δ are used in the literature, most commonly $\delta = \sqrt{2\nu/\sigma}$.

Eagleson and Dean (1959) reviewed earlier work performed by themselves and by others on discrete particle motions on roughened slopes. More recently Komar and Miller (1974) reviewed existing data on the subject, especially that due to Bagnold (1946), Manohar (1955), and Rance and Warren (1968). They derived the following empirical expressions for two domains of grain diameters;

$$\rho U_0^2/(\rho_s - \rho)gD = \begin{cases} 0.21 \ (d_0/D)^{1/2} \ ; \ D < .05 \ cm & (1.7) \\ \\ or \\ \\ 0.46 \ \pi(d_0/D)^{1/4} \ ; \ D > .05 \ cm & (1.8) \end{cases}$$

where U_0 is the external velocity $= a\sigma/\sinh kd$, d_0 is the particle excursion length at the bottom, d = water depth, and D is the sediment diameter. For prototype waves, grain diameters less than .05 cm (medium and fine sands) will be set in motion while the flow regime is laminar. They also noted that as the wave period increases, the critical value of U_0 also increases.

The development of bed forms is accompanied by "separation." Separation means that the flow becomes detached from the boundary and is a result of energy dissipation in the boundary layer. Separation of the flow along a curved boundary occurs when the deceleration of the flow necessary to maintain contact with the boundary exceeds the energy available to produce such a bending of the streamlines (Rouse, 1938). When separation occurs such that the eddy sizes are comparable to the boundary layer thickness, the flow must be considered turbulent. Jonsson (1966) has prepared a series of diagrams using existing data from which the friction factor, flow regime and boundary layer thickness can be determined for wave motions.

The effect of porous bed forms on uniform flows is just beginning to be studied. Ho and Gelhar (1973, 1974) conducted theoretical and experimental investigations for turbulent pipe flow with such a boundary. They concluded that the seepage flow in the bed can have significant influence on the external flow and therefore on the form resistance.

Theoretical consideration of turbulent flow regimes under waves is essentially limited to two papers by Kajiura (1964, 1968). In the first paper, bottom friction is studied under the assumption that the eddy viscosity coefficient is proportional to the amplitude of the bottom friction velocity and the height above the bottom, $K_z = \acute{k} (z+z_0)u_b^*$ where z_0 is the roughness length, $\acute{k}$ is von Karman's constant and u_b^* is the friction velocity. His results were utilized by Horikawa and Watanabe (1967) to aid in the prediction of the critical water depth for sediment motion. They found this approach more suitable than the previous approach which assumed the boundary layer always to be laminar and the frictional law for steady flow to remain applicable. In oscillatory flow, the friction coefficient assumes a dependence upon the phase difference between the external flow and the bottom shear stress.

$$C_f = n\tau_0/(\rho U_0^2) \tag{1.9}$$

where n must be determined experimentally.

In his second paper Kajiura introduces a more sophisticated model in which he breaks the boundary layer into three regions (inner, overlap, and outer) just as in steady turbulent flow (see Figure 1.3). Values of K_z are assumed for each region and the solutions for each section are matched. He also defined "smooth" and "rough," (see Figure 1.3). Hori-

Transition from smooth to rough $\quad 0.4 \leq D/D_L \leq 5$

D = Nikuradse's equivalent roughness

z_o = roughness length

$D = 30\, z_o$

Outer Layer

$K_z = 0.02\, U_o\, \delta^*$

δ^* = displacement thickness

U_o = magnitude of external velocity

Overlap Layer

$K_z = 0.4\, u_b^*\, z$

u_b^* = friction velocity

Viscous Sublayer

$K_z = \nu$

$D_L = 12\nu/u_b^*$

Defect Layer

Wall Layer

$d = \dfrac{0.05\, U_o\, \delta^*}{u_b^*}$
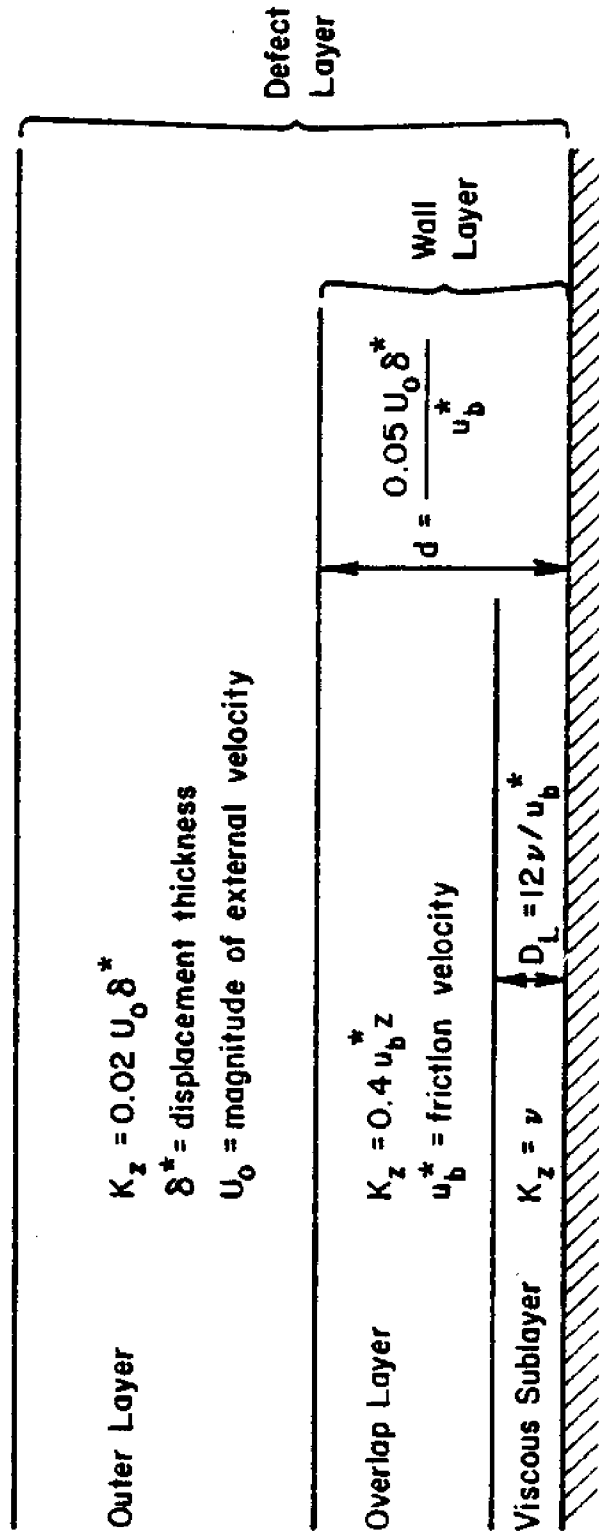
Figure 1.3 Turbulent boundary layer and Kajiura's assumptions

kawa and Watanabe (1968) compared Kajiura's results to laboratory re-
sults of their own and of Jonsson (1963). They concluded that Kajiura's
values of K_z are not always valid and that once eddies form the neglect
of the vertical velocity in the boundary layer equation is not a valid
assumption. As yet, no other turbulence model for this type of flow
has been advanced. Teleki and Anderson (1970) compared experimental
measurements of C_f to the C_f assumed by Kajiura and found n=1/2 to
give the best fit.

Two other important comments must be made with regard to the boundary
layer. Extensive laboratory tests have been made to measure wave attenua-
tion for a smooth impermeable bottom. The findings of Grosch and Lukasik
(1960), Eagleson (1962), Lukasik and Grosch (1963), and Iwagaki et al.
(1967) indicate large discrepancies between measured and theoretical val-
ues of the attenuation constant, γ , even when theoretical side wall and
surface tension effects are included. All their tests were within the do-
main of Stokian theory and under laminar conditions. Treloar and Brebner
(1974) recently developed a procedure for measuring the side-wall contribu-
tion and found it could be predicted very well. However, they were not
able to explain the fact that bottom losses are greater than theory pre-
dicts by a factor of 1.3.

The last comment concerns the continuing argument as to whether or
not oscillating bed studies are a relevant means of studying bed forms
and related flows. Einstein (1972), for one, maintains that they are
relevant, while, on the other hand, Tunstall and Inman (1975) hold that
they are not. Tunstall's data indicated that the pressure gradient field

is very important to eddy formation and therefore to the flow regime. A very good review article on the topic of wave boundary layers with respect to sediment transport has been written by Teleki (1972).

This section has been a discussion of three intertwined assumptions. These are that the boundary is smooth and stationary and that the flow is laminar and being so can be linearized. If the bed is nonrippled, the boundary will be hydrodynamically smooth for most beach and shelf sands. The roughness length will be some fraction of the grain size. Coarse sand has a maximum grain diameter of 1 mm. Therefore the minimum boundary layer thickness must be about 6 mm. A wave having a period more than 5 sec. meets this requirement and as T increases so will the value of δ. Most prototype waves of interest do have periods greater than 5 sec. The main justification of assuming a laminar oscillatory boundary layer is simply because too little is known about turbulence at the present time to include it. As commented earlier, the flow regime is most likely to be turbulent under prototype conditions when sediment motion is initiated for beds coarser than medium sand; in this case, assuming a stationary bed is consistent to a laminar boundary layer in the real world, although it may not be true in the laboratory. For beds finer than coarse sand, motion will occur under laminar conditions, but the boundary condition for a mobile bed with various degrees of sediment motion is not known and any theory, whether turbulent or laminar, is bound to be invalid when the threshold is reached. Thus we are limited to a laminar boundary layer over a stationary bed. Also, if we are limited to a laminar boundary layer, indications are that neglect of the nonlinear terms causes little error.

1.6 Porous Bed Flow

Darcy's empirical law is taken as the governing equation within the sediment layer. It was obtained during the 1850's by French hydrologist Henry Darcy while studying the water supply of Dijon, France. It can be written in its more general form as

$$\frac{1}{\nu\epsilon} (\tilde{\underline{u}}_s)_t + \frac{1}{K} \tilde{\underline{u}}_s = -\frac{1}{\mu} \underline{\nabla} (p_s - \rho gz) \quad . \tag{1.10}$$

ϵ is the porosity, K is the specific permeability, and $\tilde{\underline{u}}_s$ is the seepage velocity. $\tilde{\underline{u}}_s$ represents a mean flow rate through an infinitesmal area and is not a discrete fluid particle velocity. Porosity is simply the ratio of pore volume to total volume. The specific permeability is a proportionality constant. Its value will depend on the porosity somewhat, but more importantly on how the pores are connected and how uniformly they are dispersed. A vast number of papers have been written on applications, limitations and extensions of this equation. It assumes that the fluid is homogeneous and that the porous medium is statistically homogeneous.

Darcy assumed a linearized friction term which is fine for "slow" flows (see Table 1.3). Quadratic friction terms have been used for greater flow rates. Information given by Zaslavskii et al. (1968) for porous flows appears in Table 1.3. Therefore, one must be careful not to over-extend results obtained from this theory. The time dependent term can usually be eliminated for most natural conditions since K is $0(10^{-5})$ or less and the porosity is generally 0.4 to 0.5.

With the exception of Savage (1953), most notable works have neglected percolation effects. Vincent (1957) noted that porosity facilitated the the onset of turbulence when grain sizes were greater than 0.24 mm.

Table 1.3 Porous bed flow

$1 < \tilde{u}_s \, D/\nu < 10$	validity of Darcy's law
$\tilde{u}_s \, D/\nu < 100$	laminar flow
" > 150	turbulent flow
$10 <$ " < 100	quadratic flow law

where D = grain diameter

Putnam (1949) published the first paper on energy dissipation due to percolation and his results were corrected by Reid and Kajiura (1957). Putnam had neglected the bottom layer. Several other porous bed theories on energy dissipation which include the boundary layer are by Hunt (1959), Murray (1965), and Liu (1973). Each approach is different in that all use different matching conditions at the interface. Their results will be given in more detail later. Whether or not percolation will be an important source of dissipation depends on the depth to wave length ratio, the thickness of the bed, and the bed material. Reid and Kajiura (1957) have shown that percolation effects are the greatest for intermediate waves. In this range, the bottom pressure gradient will have its greatest values and therefore induce the largest seepage flows.

Millikan, _et al_. (1972) have explored the sediments on the eastern U. S. continental shelf and found mostly medium to coarse sands (.25 mm < D < 1 mm). Typically, the sand on the beach will not be the same as found on the shelf. Wave sorting and past geological history of

the region prevent uniformity. However, sufficiently large tracts are statistically homogeneous and allow us to consider the porosity and permeability to be constant. As the wave approaches the beach, the values of ε and K may be adjusted.

The east coast shelf is notably wide especially in the Georges Bank area off New England (over 400 km). The shelf break is seldom more than 60 m deep south of Cape Hatteras and 120 to 160 m north of Hatteras. As for the bed depth, seismic work and sediment coring on the Cape Kennedy inner shelf by Field et al. (1971) and Field and Duane (1972) show the bed depth to be highly variable there and having maximum thicknesses in the neighborhood of 40 feet. These facts indicate that waves are quite capable of transporting bottom material on this shelf when the previously discussed work of Komar et al. (1972) is considered. This is borne out in another report (Pilkey and Field, 1972), where observations are presented which indicate onshore transport of shelf sediments.

Field and laboratory experiments on porous bed effects are rare. To the author's knowledge, only one field test on wave attenuation has been published. Unfortunately, it was done in the Gulf of Mexico at a location where the bottom was cohesive mud and percolation was not a factor (Bretschneider, 1954). He believed the bottom to be somewhat fluidized by the wave action resulting in an elastic layer along the bottom. Savage (1953) has measured energy loss due to percolation in a wave tank, and Sleath (1970) has taken wave-induced pressure measurements within a stratified bed, also in a wave tank. Field measurements of seepage

velocities in the surf zone have been achieved by Reidl and Machan[1]
using hot thermister probes.

Recent geological research off the eastern and western U. S. sea-
boards has shown that significant shelf sediment transport occurs and
that the shelf material is sufficiently coarse for percolation to be a
factor in wave attenuation and to the boundary layer structure. Findings
also indicate that the material is rather constant over large areas, justi-
fying the use of a single value of K for both horizontal and vertical
directions.

In the next section, a more detailed analysis of the above mentioned
wave-porous bed models will be given.

---

[1]Riedl, R. J., R. Machan, "Hydraulic Patterns in Lotic Intertidal
Sands," (unpublished). Institute of Marine Science, Morehead City,
North Carolina, 1971, 71 p.

2   LITERATURE REVIEW

2.1   Initial Comments

In this section a review of the existing papers on wave-porous bed interactions will be made. Also, papers dealing with the "radiation-type" boundary condition utilized in this report will be discussed.

All of the porous bed models assume small amplitude wave theory or simply small amplitude motions and Darcy's law. The distinguishing feature is the manner in which the flows are coupled. The large-scale properties, i.e., streamline pattern, will not be greatly affected by the flow matching conditions since the pressure distribution will remain fairly independent of flow near the interface where viscous effects are very strong (but laminar). As for the flow near the fluid-bed interface, the matching conditions are important and the theories will always disagree in this region. Of particular importance is the shear stress, τ .

All the theories neglect all other types of interactions and therefore are subject to the limitations described in Chapter 1. Some include a damped amplitude, but others assume the amplitude loss over a wavelength to be negligible and thus take it to have a constant magnitude.

2.2   Wave-Porous Bed Models

Putnam (1949) published the first paper on this topic. He was not interested in boundary layer effects in this publication since he and Johnson (Putnam and Johnson, 1949) had already published a separate study on energy losses due to bottom friction. The purpose was merely to obtain an estimate of the energy loss due to the induced seepage flow. To accomplish this, he assumed both flows to be governed by Laplace's

equation, took the external flow to be the classical small-amplitude wave theory and solved for ϕ_s , the velocity potential in the bed, using these conditions:

$$\phi_s = gH \; coshkd \qquad\qquad z = 0 \qquad\qquad (2.1)$$

and

$$(\phi_s)_z = 0 \qquad\qquad z = -h \qquad\qquad (2.2)$$

where $\phi_s = gz + p/\rho$, d is the mean water depth, and H = wave height. The subscript 's' denotes a bed quantity and the subscript 'z' indicates differentiation with respect to the z coordinate. No viscous boundary layer is included and the external wave flow is independent of the bed flow, i.e., an uncoupled system. There is an error in equation (2.1). A divisor of 2 is missing in the denominator. This results in an overestimation of the percolation losses by a factor of four. Savage (1953) later noted a discrepancy when he compared experimental attenuation to that predicted by Putnam. The average rate of dissipation per unit length and crest width is obtained by integrating the dot product of the viscous force, $\nu\tilde{u}_s/K$, and the flow velocity, $\bar{u}_s$, over the bed thickness and the wavelength and then dividing by L.

Putnam numerically approximated the amplitude attenuation of various waves on various bottom slopes between the points d/L = 1/2 and the breaker zone. For example, on fairly flat beaches (slope 1/300), $(a_i - a_f)$ /$a_i \simeq 10\%$ for a 12 sec. wave. The subscripts 'i' and 'f' denote initial and final values, respectively. This decrease in amplitude seems rather small, but it must be remembered that waves traveling in water of

shallowing depth experience a monotonic decrease in wavelength. At the same time a monotonic increase in amplitude results once the wave enters shallow water. Had he calculated the amplitude difference on a nonsloping bottom, the percentage would have been higher, especially for intermediate depths. Also, he made another error (his eq. 18) which led him to an erroneous evaluation of the effect of bed depth. This error was found by Savage but the initial error was not found and corrected until 1957. In the meantime, his results were used and expanded by others, most notably Bretschneider and Reid (1954).

Reid and Kajiura (1957) finally recognized Putnam's most major mistake and made three improvements. (1) They coupled the flow regimes, both of which were potential flows again, with no boundary layer, (2) they included a damped free surface elevation $\eta = a_i e^{-\gamma t + ix}$, where γ · is the attenuation coefficient and (3) they included the time dependent acceleration term in Darcy's law. The matching conditions at the bottom were

$$p = p_s \quad \text{and} \quad W = \tilde{w}_s \qquad\qquad z = 0 \qquad\qquad (2.3)$$

i.e., continuous pressure and vertical velocity. The vertical velocity is zero at some finite bed depth. This approach, as with Putnam's, results in a discontinuous horizontal velocity at $z = 0$. Their method of calculating the average energy loss per unit time is to integrate the dot product of p_0 and w_0 over a period and divide by T. Several interesting phenomena resulted from the bed being porous. As with Putnam, the percolation has a negligible effect on wave length, phase speed, and group velocity. In addition, the maximum energy loss occurs at the rela-

tive depth of d/L = 0.13, which indicates waves of intermediate wave-lengths (or period) are attenuated at the highest rate by the seepage flow. The reason is that these waves induce the greatest pressure gradients at the bottom. This selective attenuation should gradually change the energy spectrum of a wave group containing many different frequencies.

Hunt (1959) was the first to include the effects of viscosity in the fluid regime. His approach was somewhat different from the usual scheme of simply correcting the external potential flow near the interface. He considered the case of small amplitude motions in a viscous fluid and therefore solved the linearized Navier-Stokes equations by defining $u = -\phi_x - \psi_z$ and $w = -\phi_z - \psi_x$. ϕ satisfies Laplace's equation and $\nu\nabla^2\psi = \psi_t$, where ψ is the stream function. At the surface, along with the kinematic condition, a vertical stress condition was used;

$$-p/\rho + 2\nu w_z = 0 \qquad\qquad z = d + \eta , \qquad (2.4)$$

while at the bottom, the vertical stress was taken to be continuous;

$$p + 2\nu w_z = p_s + 2\nu(\tilde{w}_s)_z \qquad\qquad z = 0 . \qquad (2.5)$$

The vertical velocity component is assumed continuous and the horizontal velocity component is taken to be zero. It is very unlikely that the vertical stress will be continuous across the interface. The bed is taken to be infinitely deep which is not a realistic assumption.

Hunt's conclusions are (1) the damping is essentially the sum of the boundary layer damping with an impermeable bottom and the bed damping given by Reid and Kajiura, and (2) when neither the porosity nor

the permeability are small, there are two possible wave velocities. The second result must be viewed with skepticism since Darcy's law and the boundary conditions applied would most likely fail to be valid for beds with permeabilities of that magnitude. He also found a slight increase in the wave period, T , due to the porous bottom.

Murray (1965) did an analysis similar to Hunt's in that he also solved the linearized Navier-Stokes equations over the entire fluid region and allowed the bed to be infinitely thick. The surface displacement was not damped. Unfortunately, the equation for the bed flow is not Darcy's law since the time-dependent term is multiplied rather than divided by the porosity.

Murray recognized that the stresses are not continuous across the interface and developed a new boundary condition. The criteria for this condition is that the rate of doing work should be conserved across the interface. The bottom surface is conceptualized as being a series of irregularly spaced rectangles of the same height. His condition was stated as

$$(\frac{Q_1}{Q_2}) \; \mu \; (\psi_{zz} -\psi_{xx}) - (p + 2\mu\psi_{xz}) = -p_s \qquad z = 0 \qquad (2.5)$$

where Q_1 and Q_2 are the components of the seepage flow in the x and z directions, respectively, and p and p_s are the pressures in the fluid and the bed, respectively. Neither Hunt nor Murray maintain that the two pressure fields are continuous at the interface.

Liu (1973) did a rather straightforward and uncomplicated analysis. He made a new innovation by including a non-slip condition at the interface so that both the horizontal and vertical velocity components are

continuous. The flows are governed by Laplace's equation subject to a linearized bottom boundary layer and an infinitely deep bed. The surface elevation is not considered to be damped as assumed by Reid and Kajiura, and Hunt. Therefore the attenuation coefficient has no effect on any other derived quantities. As in Hunt's paper, the vertical stress is continuous which implies that the vertical shear stress is continuous since $p = p_s$ at the bottom. The horizontal stress is also assumed to be continuous. The dispersion relationship is obtained from the linearized kinematic surface boundary condition, equation (3.9). He found the same two values for σ as Hunt had found, and the porous bed dissipation is found in a similar manner as in Putnam's paper. A comparison between theory and Savage's experiments indicated a tendency from low to high values as d/L decreases across the intermediate range. There appears to be an error in his evaluation of the boundary layer attenuation factor. The results obtained by Hough (1896) and the writer for the impermeable case are equal, and are twice that given in Liu's equation 28. No correction is made in the errata which was published in October, 1974, or in the discussion by Dalrymple (1974).

2.3 The "Radiation-Type" Condition

Beavers and Joseph (1967) published a paper which discussed a boundary condition for flow at the fluid-bed interface. It is a condition on the horizontal component and is written as

$$u_z = \frac{\alpha}{\sqrt{K}} (u - \tilde{u}_s) \qquad\qquad z = 0 , \qquad (2.6)$$

where K = permeability, u = fluid velocity, $\tilde{u}_s$ = porous bed flow, as given by Darcy's law, and α is a constant whose value depends on

the porosity. It is similar in form to the "radiation-type" boundary condition encountered in heat conduction problems. In this case, it is essentially a statement concerning the shear stress distribution across the interface. In the case of two adjacent Newtonian fluids flowing at different rates, the shear stress must be continuous since neither fluid can sustain shear stress. On the other hand, the bed is capable of sustaining a shear stress and, therefore, although the velocity profiles should be continuous, it should show a marked discontinuity in slope.

The investigators performed a series of experiments using a Poiseuille flow arrangement to test the validity of this hypothesis. They used two types of artificial beds, one "granular" and the other a "lattice-type". The fluid was a 100-grade oil. The parameter measured was the discharge, Q , from between the top plate and the bed interface. The fractional increase $\phi = (Q - Q_i)/Q_i$, between Q and the theoretical discharge for flow between two impermeable plates, Q_i , was plotted. Some of this data is reproduced in Figures 2.1 and 2.2, with an additional curve added. The additional curve is ϕ_c for the case of continuous horizontal shear (see Appendix 7.1). In Figures 2.1 and 2.2, d represents the gap between the two boundaries. For large values of $d/\sqrt{K}$ and small values of K , the separation between ϕ_c and the data is quite large. The other curves represent theoretical results using the above boundary condition. The α's shown are those which give the best fit. The values of $\alpha/\sqrt{K}$ for the curves given by Beavers range from 30 to 150 cm^{-1} and are listed in Table 2.1.

Recently three separate papers were published concerning this 'slip' condition. Saffman (1971) published a statistical analysis
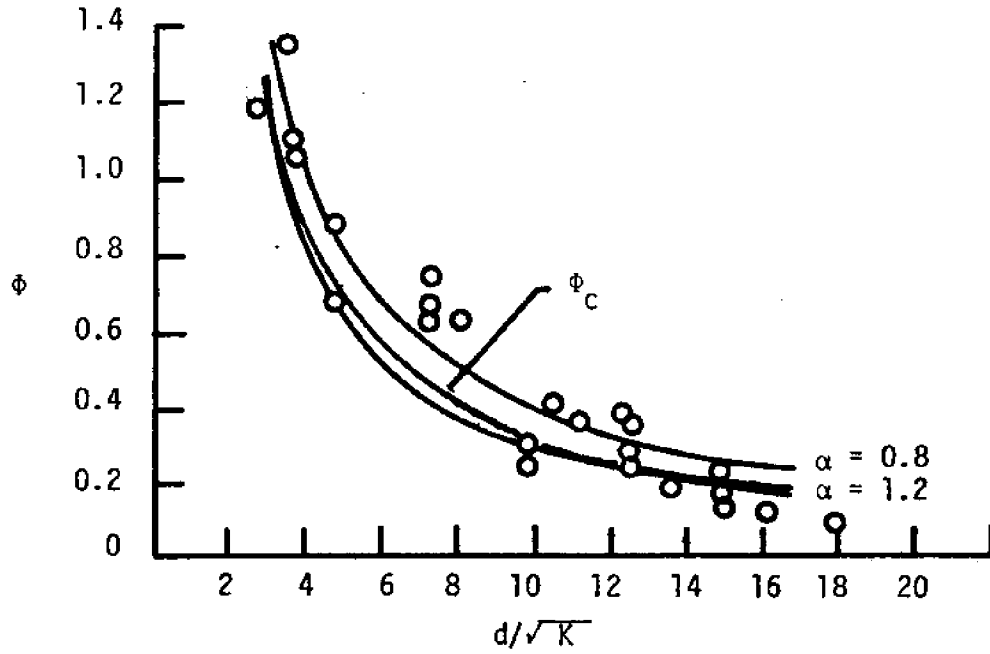
Figure 2.1 Comparison of Φ_c and data from Beavers and Joseph, (1967). $K = 7.1 \times 10^{-5}$ cm^2
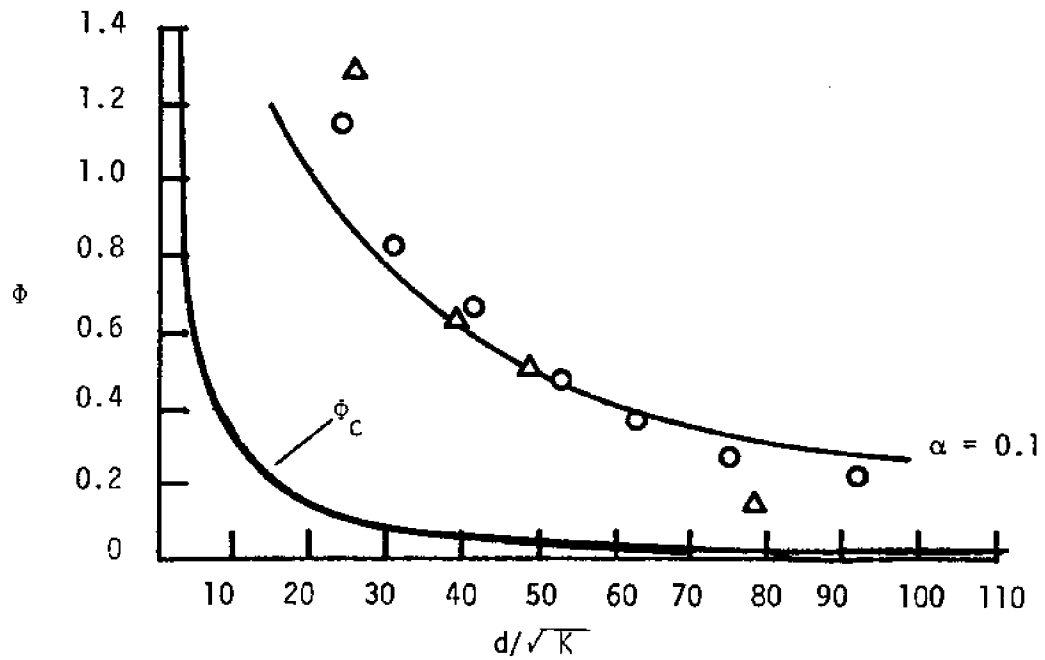
Figure 2.2 Comparison of Φ_c and data from Beavers and Joseph, (1967). o → $K = 6.5 \times 10^{-6}$ cm^2
Δ → $K = 1.6 \times 10^{-5}$ cm^2

Table 2.1.   Values of $\alpha/\sqrt{K}$ from Beavers and Joseph, (1967)

Material	$K(cm^2)$	α	$\alpha/\sqrt{K}$ (cm^{-1})
Aloxite (particulate)	1.6×10^{-5}	.10	25
Aloxite	6.5×10^{-6}	.10	39
Foametal (lattice)	8.2×10^{-4}	4	140
"	7.1×10^{-5}	1.2	142
"	7.1×10^{-5}	0.8	95
"	3.9×10^{-4}	1.45	73
"	9.7×10^{-5}	.78	79

extending Darcy's law to nonhomogeneous porous media. From the limiting case of a step function distribution of K and ε , a boundary condition very similar to Beavers' was obtained and it was suggested that the $\tilde{u}_s$ term could be dropped. Taylor (1971) published an experiential work based on the theoretical derivation of Richardson (1971). The apparatus used to test the radiation condition involved a torsion pendulum suspended above a grooved rotating plate. The plate simulated a porous bed whose porosity and permeability were determined by its design. By measuring the torque exerted on the torsion plate a comparison could be made with theoretical predictions and therefore test the condition's validity. Their results supported the hypothesis.

3 THEORETICAL DEVELOPMENT

3.1 Initial Comments

The wave-porous bed problem involves the solution of two coupled flows. The major regions are the fluid and the bed. The two boundary layers, shown in Figure 3.1, are required in order that the flows satisfy the listed physical conditions at the interface. Since viscous effects in the main body of fluid are small, the flow field can be determined from the equation of continuity which, in turn, can be expressed in terms of the velocity potential.

$$\nabla^2 \phi = 0 .$$ (3.1)

The velocity potential is defined from the relationships $U = (\phi)_x$ and $W = (\phi)_z$. U and W represent the horizontal and vertical velocity components of the wave field. The subscripts, x and z, indicate differentiation with respect to the two coordinates. Equation (3.1) is Laplace's equation. One condition at the surface and one condition at the bottom can be satisfied by the solution of Laplace's equation. The remaining condition at the surface is satisfied by relating σ, the frequency, to k, the wave number, in terms of physical quantities such as the water depth, d. This relationship, called the dispersion relationship, governs the possible combinations of these two wave parameters.

Darcy's law, shown in Figure 3.1, expresses a linear dependence between the seepage flow and the pressure gradient. The quantities $\tilde{u}_s$ and $\tilde{w}_s$ will be used to denote the horizontal and vertical components

$$\frac{\partial \phi}{\partial z} = \frac{\partial \eta}{\partial t} \quad \text{kinematic}$$

$$\frac{\partial \phi}{\partial t} = -g\eta \quad \text{dynamic}$$

MWL

$\nabla^2 \phi = 0$

η

d

$u = u_s$
$w = w_s$
$p = p_s$
$\left.\dfrac{\partial u}{\partial z}\right|_0 = \dfrac{a}{\sqrt{K}}(u - \tilde{u}_s)$

B.L. #1

x

$$\frac{\partial u}{\partial t} - \nu \frac{\partial^2 u}{\partial z^2} = -\frac{1}{\rho}\frac{\partial p}{\partial x}$$

B.L. #2

$$\frac{\partial^2 u_s}{\partial z^2} + \frac{\partial^2 u_s}{\partial x^2} - \frac{1}{\nu_\epsilon}\frac{\partial u_s}{\partial t} - \frac{1}{K}u_s = \frac{1}{\mu}\frac{\partial}{\partial x}(p_s - \rho g z)$$

Darcy's law:
$$\frac{1}{\nu_\epsilon}\frac{\partial \tilde{u}_s}{\partial t} - \frac{1}{K}\tilde{u}_s = -\frac{1}{\mu}\nabla(\bar{p}_s - \rho g z)$$

z

h
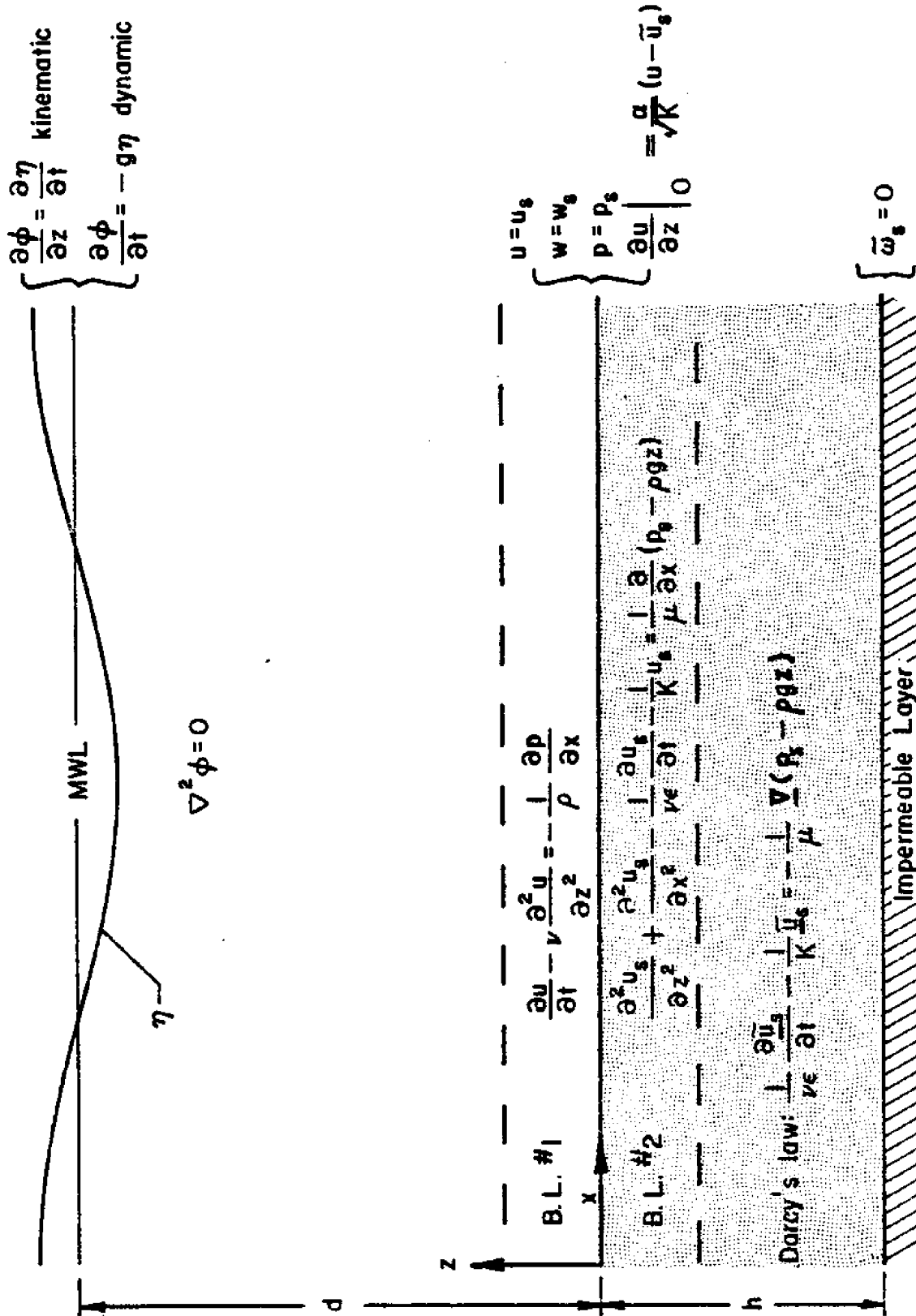
Impermeable Layer

$\tilde{w}_s = 0$

Figure 3.1   Equations of motion and boundary conditions

of the seepage flow as derived from Darcy's law. The subscript "s" will denote a sediment-related quantity. No such subscript is used with the fluid-related quantities. The seepage velocity in Darcy's law is a statistical mean discharge per unit area. Conceptually, the flow in the bed is treated as if it were a single phase media. This approach is justified since the velocities under consideration are averages and do not represent the real interstitial flow within the pores of the bed. Thus the velocity field is seen as having a value at all points in the bed, whereas in reality, the flow is nonexistent within the sediment particles.

3.2 Solution for the Potential Field

In this section, the solution for the flow in the main body of the fluid is found. The kinematic boundary condition at the surface will be applied, but application of a bottom boundary condition must wait until the solutions for the bed and boundary layer flows have been derived.

As mentioned in section 1.4, the exact solution of Laplace's equation subject to conditions (1.4), (1.5), and (1.6) is not known and requires the use of an approximation method. Of course, equation (1.6) will be replaced with a nonhomogeneous condition because of the vertical flow through the permeable interface. ϕ and η, the vertical surface displacement, are expanded into perturbation series,

$$\phi = \hat{\epsilon}\, \phi_1 + \hat{\epsilon}^2\, \phi_2 + \cdots \tag{3.2}$$

and

$$\eta = \hat{\epsilon}\, \eta_1 + \hat{\epsilon}^2\, \eta_2 + \cdots \tag{3.3}$$

where the expansion parameter, $\hat{\epsilon}$, is assumed to be small relative to unity. For small amplitude waves, it will be shown in Chapter 4 that $\hat{\epsilon}$ is of the order 'ak' where 'a' is the wave amplitude. η represents the surface elevation with respect to the mean water level, d. The boundary conditions at the surface are given as

$$\eta_t + U \cdot \eta_x = W = \phi_z \quad \text{(kinematic)} \quad z = \eta + d , \tag{3.4}$$

$$\phi_t + (1/2) (\phi_x^2 + \phi_z^2) + gz = 0 \quad \text{(dynamic)} \quad z = \eta + d, \tag{3.5}$$

where the subscript "t" denotes differentiation with respect to time.

Since η is not known, the evaluation of ϕ or any of its derivatives at $z = \eta + d$ must be approximated using a Taylor's expansion about $z = d$.

$$\phi|_{d+\eta} = \phi|_d + (\eta-d) \phi_z|_d + \cdots \tag{3.6}$$

where "$|_d$" indicates the evaluation of the function at point $z = d$.

The perturbation expansion of ϕ is substituted into the Taylor's expansion of $\phi|_{d+\eta}$. The resulting expression is substituted into the surface boundary conditions, (3.4) and (3.5). The first-order boundary conditions are obtained by retaining only the terms having $\hat{\epsilon}$ as a coefficient.

$$(\phi_1)_z = (\eta_1)_t \quad \text{(kinematic)} \quad z = d \tag{3.7}$$

and

$$(\phi_1)_t = -g\eta_1 \quad \text{(dynamic)} \quad z = d . \tag{3.8}$$

The implementation of the perturbation series has resulted in the linearization of the surface conditions. Since only the first-order solution is considered in this paper, the subscript "1" will be dropped for the

sake of simplicity and all quantities derived are understood to be first-order approximations.

The solution sought is periodic and therefore ϕ is assumed to be

$$\phi = (A_1 \cosh kz + B_1 \sinh kz) \, e^{i\chi} \qquad (3.9)$$

where $\chi = kx - \sigma t$. x is the horizontal coordinate and the wave is propagating in the positive x direction.

Substituting ϕ and η into (3.8), the following relation between the integration constants is obtained.

$$A_1 + B_1 \coth kd = \frac{-ia\sigma}{k\sinh kd} \, . \qquad (3.10)$$

The condition at the bottom is that the horizontal and vertical velocity components are continuous . The conditions cannot be applied until the general solutions for the bed flow and boundary layer motions are obtained since the flows are coupled. Expressions for U and W can be obtained by differentiating ϕ with respect to x and z , respectively.

$$U = ik(A_1 \cosh kz + B_1 \sinh kz) \, e^{i\chi} \qquad (3.11a)$$

and

$$W = k \, (A_1 \sinh kz + B_1 \cosh kz) \, e^{i\chi} \, . \qquad (3.11b)$$

The pressure is related to ϕ using the linearized Bernoulli equation.

$$p = -\rho\phi_t + \rho g \, (z-d) \qquad (3.12a)$$

or

$$p = ip\sigma(A_1\cosh kz + B_1\sinh kz)e^{iX} + \rho(z-d)g \qquad (3.12b)$$

where ρ is the fluid density and g is the acceleration of gravity.

3.3 Solution to the Porous Bed Flow

Darcy's law, as stated below, is usually solved as a potential flow problem (Zaslavskii, et al., 1968) using the relations

$$\frac{1}{\nu\epsilon}(\tilde{u}_s)_t + \frac{1}{K}\tilde{u}_s = -\frac{1}{\mu}(p_s - \rho g z)_x = U_s \qquad (3.13)$$

and

$$\frac{1}{\nu\epsilon}(\tilde{w}_s)_t + \frac{1}{K}\tilde{w}_s = -\frac{1}{\mu}(p_s - \rho g z)_z = W_s \qquad (3.14)$$

where ν is the kinematic viscosity, μ is the dynamic viscosity, ϵ is the porosity, and K is the permeability. Since continuity must also apply to the bed, $(\tilde{u}_s)_x + (\tilde{w}_s)_z = 0$. It follows that $(U_s)_x + (W_s)_z = 0$. From (3.13) and (3.14), it is seen that U_s and W_s are expressed as the gradient of a function. Therefore, let

$$U_s = (\phi_s)_x \quad \text{and} \quad W_s = (\phi_s)_z \quad . \qquad (3.15)$$

Substitution of (3.15) into the continuity equation implies $\nabla^2\phi_s = 0$. Substituting (3.15) into (3.13) and integrating over x, we find

$$\phi_s = -\frac{1}{\mu}(p_s - \rho g z) + D_2 \quad . \qquad (3.16)$$

Let

$$\phi_s = (A_2 e^{kz} + B_2 e^{-kz})e^{iX} + G(z) \quad . \qquad (3.17)$$

From Laplace's equation,

$$G(z) = C'z + D' .$$

<div align="right">(3.18)</div>

The condition at $z = 0$ to be satisfied by this flow is continuity of pressure. The potential pressure field is assumed to be undiminished across the boundary layer. To prove this point, the vertical momentum equation must be considered since it contains the $(p)_z$ term. The usual approach (Schlichting, 1968) is to nondimensionalize the momentum equations and show that all the terms in the z equation which contain w are small compared with the terms in the x equation. If this is so, $(p)_z$ equals the sum of a number of small terms and is therefore small itself. In this case, the situation is somewhat different since percolation across the interface is allowed. However, the seepage velocity is determined by the ratio, K/μ , which has a maximum value of 10^{-3} cm^3 · sec/gr. The increase in w at the interface over the value of zero for the impermeable case remains small compared to U_o and the standard boundary layer approximations remain valid. The subscript "o" denotes evaluation at $z = 0$. Thus,

$$\phi_s\big|_o = (A_2+B_2)e^{iX} + D' = p_s\big|_o$$

<div align="right">(3.19)</div>

$$p_s\big|_o = \frac{-i\sigma A_1}{\nu} \cdot e^{iX} + \frac{gd}{\nu} + D_2 .$$

<div align="right">(3.20)</div>

Combining (3.19) and (3.20),

$$A_2 + B_2 = \frac{-i\sigma A_1}{\nu}$$

<div align="right">(3.21)</div>

and

$$D^{'} = \frac{gd}{\nu} + D_2 \quad .$$

(3.22)

In order to apply the boundary condition at $z = -h$, an expression for $\tilde{w}_s$ must be obtained. This is achieved by solving (3.14).

$$\tilde{w}_s = (\ (w_s)_i + \nu\varepsilon \int_0^t e^{\nu\varepsilon t/K} (\phi_s)_z dt) \cdot e^{-\nu\varepsilon t/K} \quad .$$

(3.23)

If we assume that the motion is initially zero, $(\tilde{w}_s)_i$ can be dropped. Performing the integration results in the following expression for $\tilde{w}_s$.

$$\tilde{w}_s = \frac{k\nu\varepsilon K}{(\nu\varepsilon - i\sigma K)} (A_2 e^{kz} - B_2 e^{-kz}) \ e^{iX} + KC^{'} \quad .$$

(3.24)

The condition at $z = -h$ is $\tilde{w}_s = 0$. Application of this condition results in two expressions.

$$A_2 e^{-kh} - B_2 e^{kh} = 0$$

(3.25)

and

$$C^{'} = 0 \quad .$$

From (3.16), (3.17), (3.18), and (3.22),

$$p_s = -\mu(A_2 e^{kz} + B_2 e^{-kz}) \ e^{iX} + \rho g(z-d)$$

(3.26)

and from continuity,

$$\tilde{u}_s = \frac{ik\nu\varepsilon K}{(\nu\varepsilon - i\sigma K)} (A_2 e^{kz} + B_2 e^{-kz}) e^{iX} \quad .$$

(3.27)

At this point, we return to the fluid regime and solve the boundary layer equations.

3.4 Boundary Layer No. 1

As discussed in the introduction, a linearized laminar boundary layer is assumed. The criteria for this assumption is strongly dependent on the expansion parameter, $\hat{\varepsilon}$, and will be derived in Chapter 4 once the solutions are obtained. The x-momentum equation is

$$u_t - \nu u_{zz} = -\frac{1}{\rho} p_x = \phi_{xt} \ . \tag{3.28}$$

If $u = \phi_x + u'$, (3.28) becomes

$$u'_t - \nu u'_{zz} = 0 \ . \tag{3.29}$$

The decomposition of u into a potential component plus a viscous correction term, u', is discussed in Phillips (1969). As z increases away from the interface, viscous effects decrease to an insignificant amount which implies that u' approaches zero. The solution to (3.29) is

$$u' = A_1' e^{(i-1)bz + i\chi} \ . \tag{3.30}$$

where

$$b = + \sqrt{(\sigma/2\nu)} \ .$$

The condition at z = 0 is the "radiation-type" condition described in Chapter 2. When the decomposition of u is employed,

$$u'_z = \frac{\alpha}{\sqrt{K}} (u' + U - \tilde{u}_s) - U_z \qquad z = 0 \ . \tag{3.31}$$

Substituting the expressions for u', $\tilde{u}_s$, and U into (3.31) and evaluating at $z = 0$ yields the condition

$$\frac{ik\alpha}{\sqrt{K}} A_1 - ik^2 B_1 + (\frac{\alpha}{\sqrt{K}} + \frac{(1-i)b}{l}) A_1' - \frac{\lambda\alpha}{\sqrt{K}} (A_2 + B_2) = 0 \quad (3.32)$$

where $\lambda = \frac{ik\nu\epsilon K}{(\nu\epsilon - i\sigma K)}$.

An expression for w' is obtained from continuity;

$$w' = \frac{iku'}{(1-i)b} \quad . \quad (3.33)$$

3.5 Boundary Layer No. 2

One of the implications involved with the "radiation-type" boundary condition at $z = 0$ is that viscous effects diffuse at least a small distance into the bed. The extent of this viscous penetration depends on the permeability and porosity. Although this distance is probably very small for the bed materials under consideration, the effect on the shear stress may prove to be significant. As mentioned in section 3.1, the matching of the horizontal velocities at the interface is consistent with the idealized bed flow. Introduction of this matching layer is necessary since both A_2 and B_2 have been utilized in two other conditions, (3.21) and (3.25). The matching layer adds another integration constant which makes the total number of constants equal to the number of boundary conditions (not including the dynamic surface condition). As in boundary layer No. 1, viscous effects decrease away from the interface and approach zero at some distance away from the bottom.

The equation utilized in boundary layer No. 2 is a result derived by Brinkman (1947) for a field of closely packed spheres. This equation has been discussed by Batchelor (1974) and is written below.

$$(u_s)_{zz} + (u_s)_{xx} - \frac{1}{\nu\varepsilon} (u_s)_t - \frac{1}{K} u_s = \frac{1}{\mu} (p_s - \rho gz)_x \ . \tag{3.34}$$

(3.34) is the horizontal momentum equation. The vertical equation has a similar form with the differentiation of the pressure term being with respect to z rather than x. If u_s is decomposed in the same manner as u, i.e., $u_s = \tilde{u}_s + u_s'$, (3.34) becomes

$$(u_s')_{xx} + (u_s')_{zz} - \frac{1}{\nu\varepsilon} (u_s')_t - \frac{1}{K} u_s' = 0 \ . \tag{3.35}$$

The condition to be satisfied at $z = 0$ is

$$u_s' = U + u' - \tilde{u}_s \ . \tag{3.36}$$

Equation (3.35) can be simplified by making use of the phase relation between x and t. Since we are dealing with trigonometric functions having χ in their arguments, a relationship between $\partial^2/\partial x^2$ and $\partial^2/\partial t^2$ exists and is stated below.

$$(k/\sigma)^2 \partial^2/\partial t^2 = \partial^2/\partial x^2 \ . \tag{3.37}$$

Using (3.37) and applying a Fourier sine transformation on (3.35) results in

$$f'' - (\frac{\sigma}{k})^2 \frac{f'}{\nu\varepsilon} - (\frac{\sigma}{k})^2 (r^2 + \frac{1}{K})f = -\Omega r e^{i\chi}$$

$$= - (\frac{\sigma}{k})^2 r(ikA_1 + A_1' - \lambda(A_2 + B_2))e^{i\chi} \ . \tag{3.38}$$

Here f is the Fourier sine transform of u_s' and r is the transform parameter. The apostrophes denote differentiation. The terms enclosed in parentheses on the right-hand side of (3.38) represent the value of u_s' at $z = 0$ as determined by matching velocities. (3.38) is a linear, nonhomogeneous, second-order differential equation in time. The complimentary solution is the sum of two exponential functions, one of which is decaying and the other grows in time. f is bounded, which eliminates the latter. Since we are not interested in transient effects, we will consider the time to be large enough to cause the complimentary solution to be insignificant in comparison to the particular integral.

The particular integral is

$$f = \frac{\Omega r e^{iX}}{(\sigma^2 - \beta i \sigma + c)} \tag{3.39}$$

where $\beta = (\frac{\sigma}{k})^2 \cdot (\frac{1}{\nu \varepsilon})$ and $c = (\frac{\sigma}{k})^2 \cdot (r^2 + \frac{1}{k})$. The inverse is given by

$u_s' = \frac{2}{\pi} \int_0^\infty f \sin (rz) dr$, which can be evaluated as

$$u_s' = (\frac{k}{\sigma})^2 \Omega e^{\theta z + iX} \tag{3.40}$$

where $\theta = (k^2 - \frac{\sigma i}{\nu \varepsilon} + \frac{1}{k})^{1/2}$, (De Haan, 1858). Using the continuity equation,

$$w_s' = \frac{-iku_s'}{\theta} \tag{3.41}$$

which allows the last remaining condition, that of a continuous mass flux across the interface, to be satisfied.

$$W_0 + w_0' - \tilde{w}_s|_0 - w_s'|_0 = 0$$

or

$$- \frac{k^2}{\theta} A_1 + kB_1 + ik \left(\frac{1}{\theta} + \frac{1}{(1-i)b}\right) A_1' + i\lambda(1 - \frac{k}{\theta}) A_2$$

$$- i\lambda(1 + \frac{k}{\theta}) B_2 = 0 . \tag{3.42}$$

Conditions (3.10), (3.21), (3.25), (3.32) and (3.42) supply the information needed to find the values of A_1, B_1, A_2, B_2, and A_1' , which are the only remaining constants found in the expressions for the various velocity components. The values of these constants are listed in Table 3.1. $\bar{A}$ represents the augmented coefficient matrix.

Table 3.1 Values of the constants of integration

1. $\text{Det }\bar{A} = 2k\cosh kh\ \{(\ \frac{\alpha}{\sqrt{K}} + (1-i)b - k^2(\frac{1}{(1-i)b} + \frac{1}{\theta})\ ) + \coth kd\ (\frac{(1-i)b}{\theta} - \frac{\alpha}{\sqrt{K}(1-i)b})\ (k + \frac{\lambda\sigma}{\nu})\}$

$- \frac{2\lambda\sigma}{\nu}(\ \frac{\alpha}{\sqrt{K}} + (1-i)b)\ \coth kd \cdot \sinh kh$

2. $A_1 \cdot \text{Det }\bar{A} = \frac{2a\sigma i}{\sinh kd}\ \{k^2(\frac{1}{(1-i)b} + \frac{1}{\theta}) - (\ \frac{\alpha}{\sqrt{K}} + \frac{(1-i)b}{\nu})\ \}\ \cosh kh$

3. $B_1 \cdot \text{Det }\bar{A} = \frac{2a\sigma^2 i}{\nu\sinh kd}\ \{((\lambda + \frac{\nu k}{\sigma})\ (\ \frac{\alpha}{\sqrt{K}(1-i)b} - \frac{(1-i)b}{\theta})\ \cosh kh + \frac{\lambda}{k}\ (\ \frac{\alpha}{\sqrt{K}} + (1-i)b)\ \sinh kh\}$

4. $A_1' \cdot \text{Det }\bar{A} = \frac{2a\sigma^2}{\nu\sinh kd}\ \{(\frac{k^2\lambda}{\theta} - \frac{\lambda\alpha}{\sqrt{K}} - \frac{\alpha\nu k}{\sigma\sqrt{K}} + \frac{k^3\nu}{\sigma\theta})\ \cosh kh - k\lambda\sinh kh\}$

5. $\frac{A_2 \cdot \text{Det }\bar{A}}{e^{kh}} = \frac{B_2 \cdot \text{Det }\bar{A}}{e^{-kh}} = \frac{-a\sigma^2}{\nu\sinh kd}\ (\ \frac{\alpha}{\sqrt{K}} + (1-i)b - \frac{k^2}{(1-i)b} - \frac{k^2}{\theta}\ )$

and

6. $A_2' \cdot \text{Det }\bar{A} = \{(\frac{a\lambda\sigma^2 k^2}{\nu}(\frac{k^2}{\theta} - \frac{\alpha}{\sqrt{K}}) + (2k + \frac{\sigma\lambda}{\nu})(a\sigma(1-i)b - \frac{a\sigma k^2}{(1-i)b}))\frac{\cosh kh}{\sinh kd} - \frac{2a\sigma^2 k\lambda\ \sinh kh}{\nu\ \sinh kd}\}$

$b = (\sigma/2\nu)^{1/2},\ \lambda = \frac{ikK\nu\epsilon}{(\nu\epsilon - iK\sigma)},\ \theta = (\frac{1}{K} - \frac{i\sigma}{\nu\epsilon})^{1/2}$

4 DISCUSSION

4.1 Initial Comments

Knowing the solutions and the integration constants, it is now possible to derive expressions for the physical quantities of interest. As seen in Table 3.1, the integration constants are quite lengthy and contain real and imaginary components. For natural conditions, quite a number of simplifications can be made with the establishment of the appropriate criteria. Appendix 7.2 lists the parameters appearing in the integration constants with their orders of magnitude. In the following derivations, the calculations are usually long involving much algebra. It serves no purpose to reproduce them here. The procedure in all derivations is to find the quantity in terms of A_1', B_1, A , A_2 and B_2, separate the real from the imaginary components and finally simplify the result using Appendix 7.2. Therefore, no approximations are made until the final result is obtained.

4.2 Potential Field Results--Fluid Regime

The velocity potential, ϕ , is found to be essentially the same as given by Airy wave theory for natural conditions. The sinhkz term is due to the porous bed modification of ϕ and approaches the value zero as $z \to 0$.

$$\phi = \frac{a\sigma}{k} \left\{ \frac{\cosh kz \cdot \sin \chi}{\sinh kd} - \frac{(J^2 + I^2)^{1/2}}{I} \left(\frac{\sigma \sqrt{K} \ \text{sechkh}}{\alpha \nu \xi \ \sinh kd} \right) \sinh kz \right.$$

$$\left. \cdot \sin (\chi + \Theta^* + \Psi) \right\} , \qquad (4.1)$$

where

$$I = -\left(\frac{\alpha k \nu}{2b\sqrt{K}\,\sigma} \cdot \cosh kh + K\left(\frac{\alpha}{\sqrt{K}} + b\right) \sinh kh\right)$$

$$J = -\left(\frac{\alpha k \nu}{2b\sqrt{K}\,\sigma} \cdot \cosh kh + Kb \sinh kh\right)$$

$$\xi = \left(1 + \frac{2b\sqrt{K}}{\alpha} + 2\left(\frac{b}{\alpha}\right)^2 K\right)^{1/2}$$

$$\theta^* = \operatorname{atan}(b/(\alpha/\sqrt{K} + b))$$

and

$$\Psi = \operatorname{atan}(I/J) = \operatorname{atan}(|I|/|J|) + \pi$$

The horizontal and vertical potential velocities can be obtained by differentiating ϕ with respect to x and z respectively. The ratio of the first term to the second term of ϕ can be shown to be of the order of $b/k \approx L/\delta \gg 1$. For this reason and also the fact that the second term of ϕ vanishes at $z = 0$, the expression for U is approximately

$$U = \frac{a\sigma \cosh kz}{\sinh kd} \cdot \cos\chi \ . \tag{4.2}$$

Since the vertical velocity at $z = 0$ is of interest the minor term of ϕ will not be dropped from W.

$$W = a\sigma\left\{\frac{\sinh kz}{\sinh kd} \cdot \sin\chi - \frac{(J^2+I^2)^{1/2}}{1}\left(\frac{\sigma\sqrt{K}\,\operatorname{sech}kh}{\alpha\nu\xi\,\sinh kd}\right) \cdot \cosh kz\right.$$

$$\left. \cdot \sin(\chi+\theta^*+\psi)\right\} \ . \tag{4.3}$$

The pressure distribution remains unaffected by the porous bed since ϕ is virtually the same as in the impermeable bed case. The pressure is written as $p = -\rho\phi_t + \rho g(z-d)$ or

$$p = \rho \frac{a\sigma^2 \cosh kz}{k \sinh kd} \cdot \cos\chi + \rho g(z-d) . \tag{4.4}$$

This result supports the approach of Putnam (1949), who left the bed and fluid motions uncoupled and simply used the pressure field of an Airy wave to drive the bed flow.

Now that an expression for ϕ has been obtained, the value of $\hat{\epsilon}$ can be derived by comparing the magnitudes of the linear terms and the non-linear terms in (3.5), i.e, dynamic boundary condition. When this is done, it is found that $\hat{\epsilon} \approx \phi_x^2 / \phi_t \approx ak$. Therefore this wave theory is valid for $ak \ll 1$, i.e., the amplitude is much smaller than the wavelength. It is also because of this fact that the nonlinear terms can be dropped from the laminar boundary layer equations.

4.3 Potential Field Results--Porous Bed

The value of ϕ_s is the same as Putnam (1949), notwithstanding his afore-discussed error.

$$\phi_s = -\frac{a\sigma^2 \cosh k(z+h)\cos\chi}{\nu k \sinh kd \cdot \cosh kh} + \frac{gd}{\nu} , \tag{4.5}$$

$$p_s = \frac{\rho a\sigma^2 \cosh k(z+h)\cos\chi}{k \sinh kd \cdot \cosh kh} + \rho g(z-d) , \tag{4.6}$$

$$\tilde{u}_s = \frac{a\sigma^2 K \cosh k(z+h)\sin\chi}{\nu \sinh kd \cdot \cosh kh} , \tag{4.7}$$

and

$$\tilde{w}_s = \frac{-a\sigma^2 K \sinh k(z+h)\cos\chi}{\nu \sinh kd \cdot \cosh kh} \; . \tag{4.8}$$

The reader should recall that z is negative in the bed.

4.4 Boundary Layer Results

The result for u´ is

$$u´ = - \frac{a\sigma e^{-bz}}{\xi \sinh kd} \cdot \cos \left(\chi + bz + \Theta^*\right) \; . \tag{4.9}$$

Since a decrease in $\alpha/\sqrt{K}$ indicates less resistance to the boundary layer flow as seen from the boundary condition, it will affect a decrease in u´. Therefore u = U + u´ increases in magnitude as does the phase advance, Θ^* , because U and u´ have opposite signs.

$$w´ = \frac{a\sigma k e^{-bz}}{\sqrt{2}\xi b \sinh kd} \cdot \cos(\chi + bz + \Theta^* - \pi/4) \; . \tag{4.10}$$

Comparing w´ to u´ , it is seen that u´ is greater by a factor of approximately L/δ .

Figures 4.1 and 4.2 show the boundary layer profiles for two different values of $\alpha/\sqrt{K}$. There is an appreciable difference between the two examples in the lower section of the layer. Note the value of u_o . To illustrate another trend, Figure 4.3 plots u_o/U_o over a wave period. Finally, Figure 4.4 shows the dependence of u_o on the phase angle χ . As $\alpha/\sqrt{K}$ decreases, there is a steady phase advance which can be substantial for small values of $\alpha/\sqrt{K}$. The program, UBLI, given in Appendix 7.3, can be used to calculate the boundary layer profiles at various values of χ .

η = SURFACE PROFILE

51
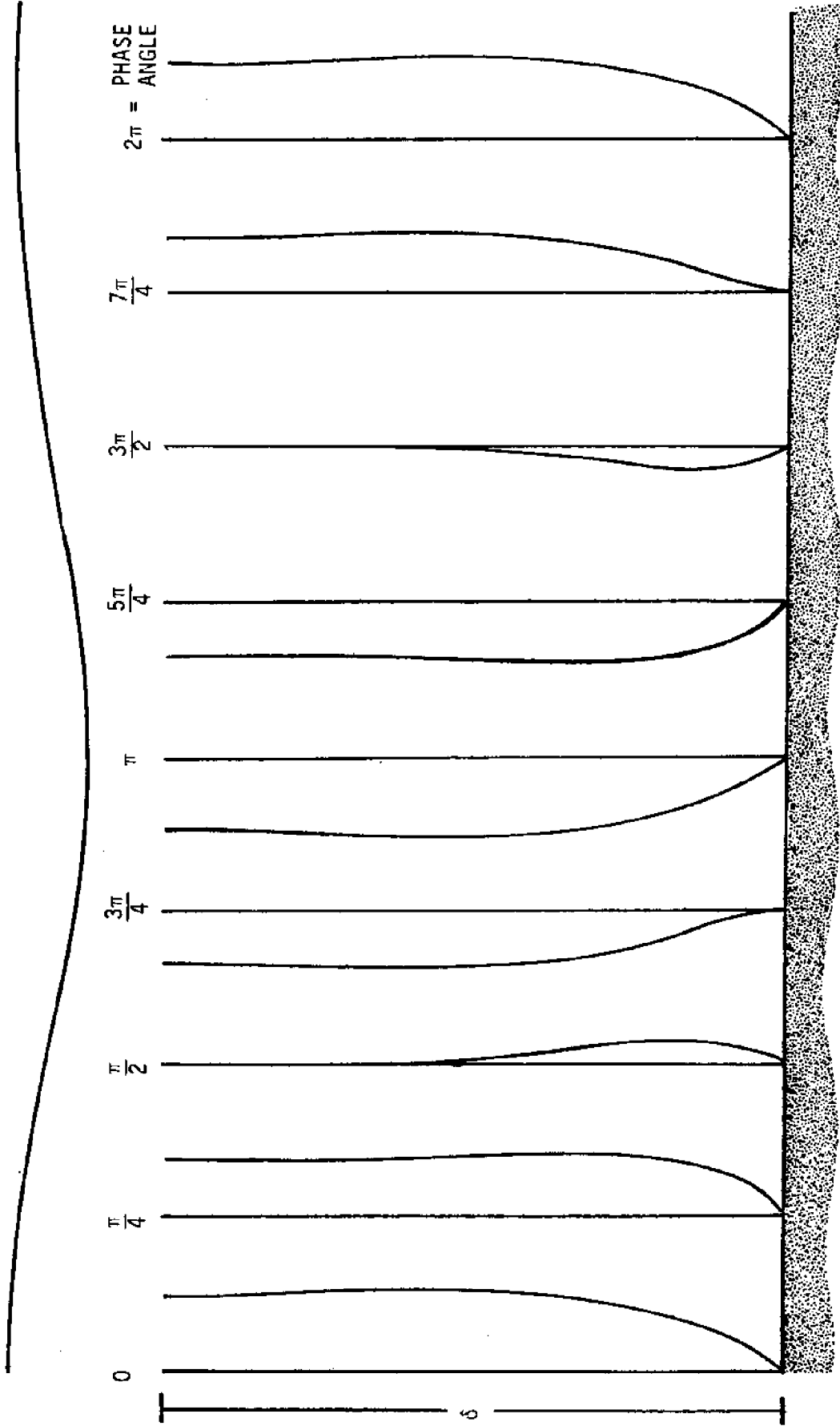
Figure 4.1. Boundary layer profiles, u/U_0, Period = 8sec., $\alpha/\sqrt{K} = 100/cm$, $\nu = 0.01$ cm^2/sec
($U_0 = a\sigma/\sinh kd$ = maximum bottom velocity predicted by potential theory)

2π = PHASE ANGLE

$\frac{7\pi}{4}$

$\frac{3\pi}{2}$

$\frac{5\pi}{4}$

π

$\frac{3\pi}{4}$

$\frac{\pi}{2}$

$\frac{\pi}{4}$

0

δ

52
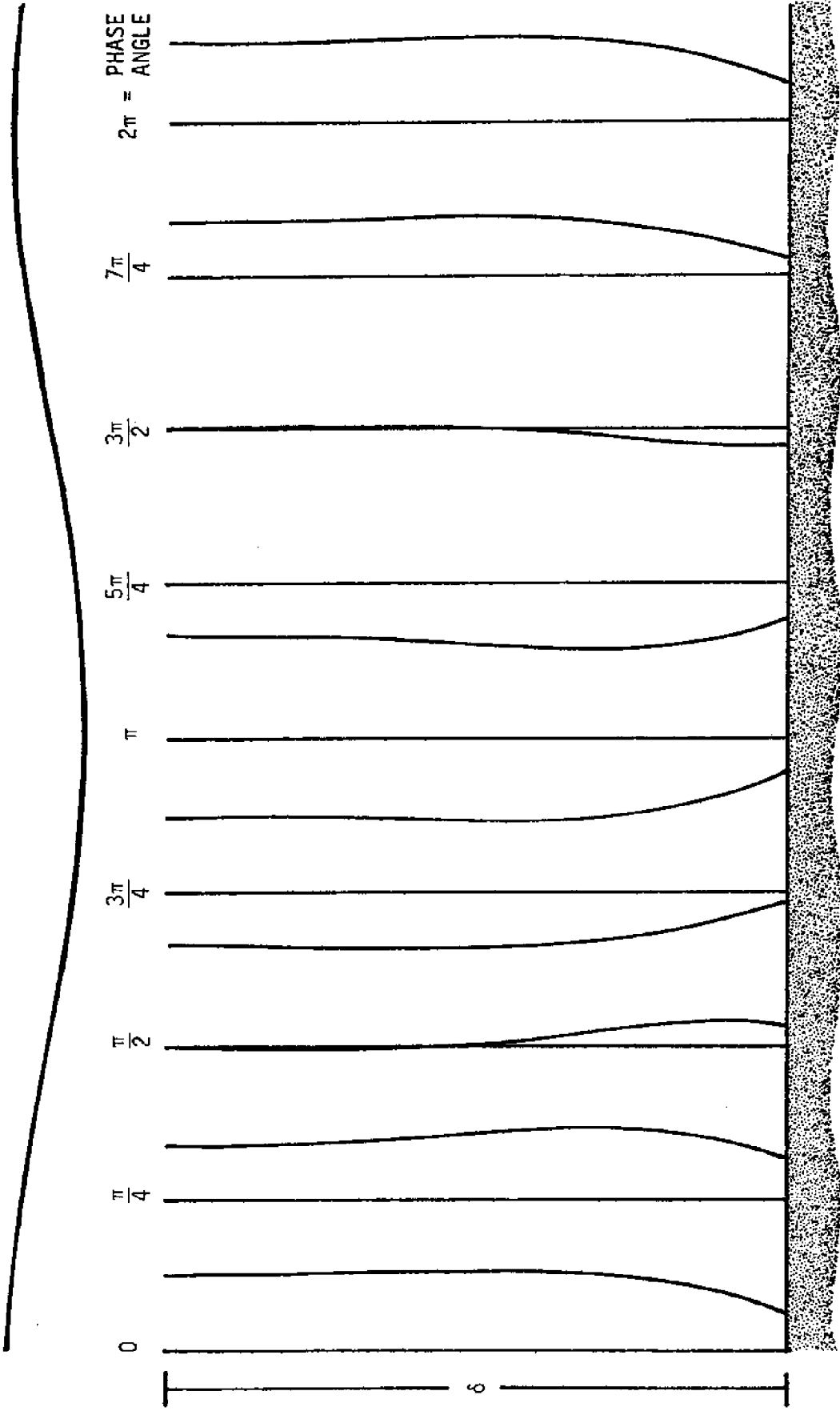
Figure 4.2. Boundary layer profiles, u/U_0, Period = 8 sec., $\alpha/\sqrt{K}$ = 10/cm, ν = 0.01 cm^2/sec ($U_0 = a\sigma/\sinh kd$ = maximum bottom velocity predicted by potential theory)

Figure 4.3 $u_0(max)\ /U_0$ vs wave period. Curves represent constant values of $\alpha/\sqrt{K}$ (cm^{-1}), $\nu = .01$ cm^2/sec

Figure 4.4 Relative bottom velocity vs phase angle curves for values of $\alpha/\sqrt{K}$ (cm^{-1}), T = 8 sec, ν = .01 cm^2/sec

The boundary layer thickness is a function of the period

$(\delta \propto \sqrt{2\nu/\sigma}\,)$. Figure 4.5 shows that short period waves have a

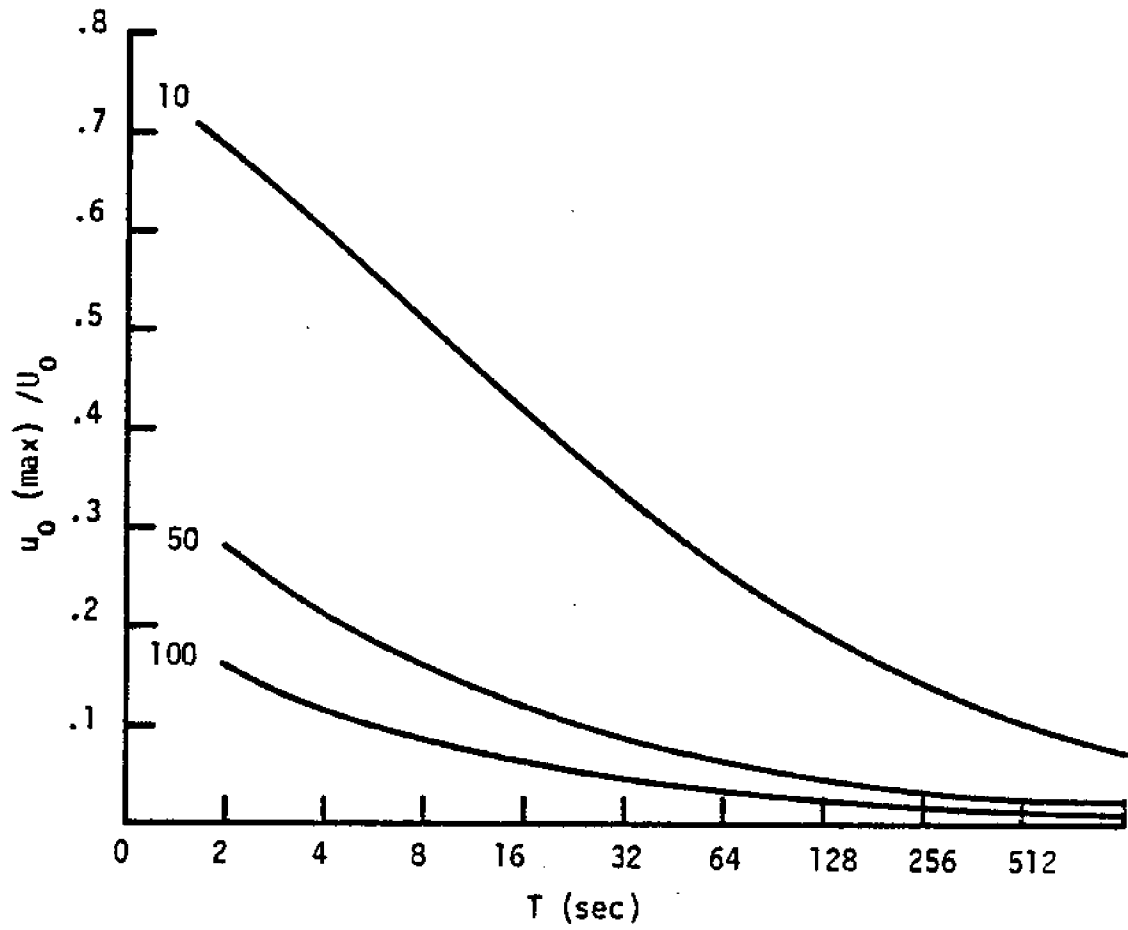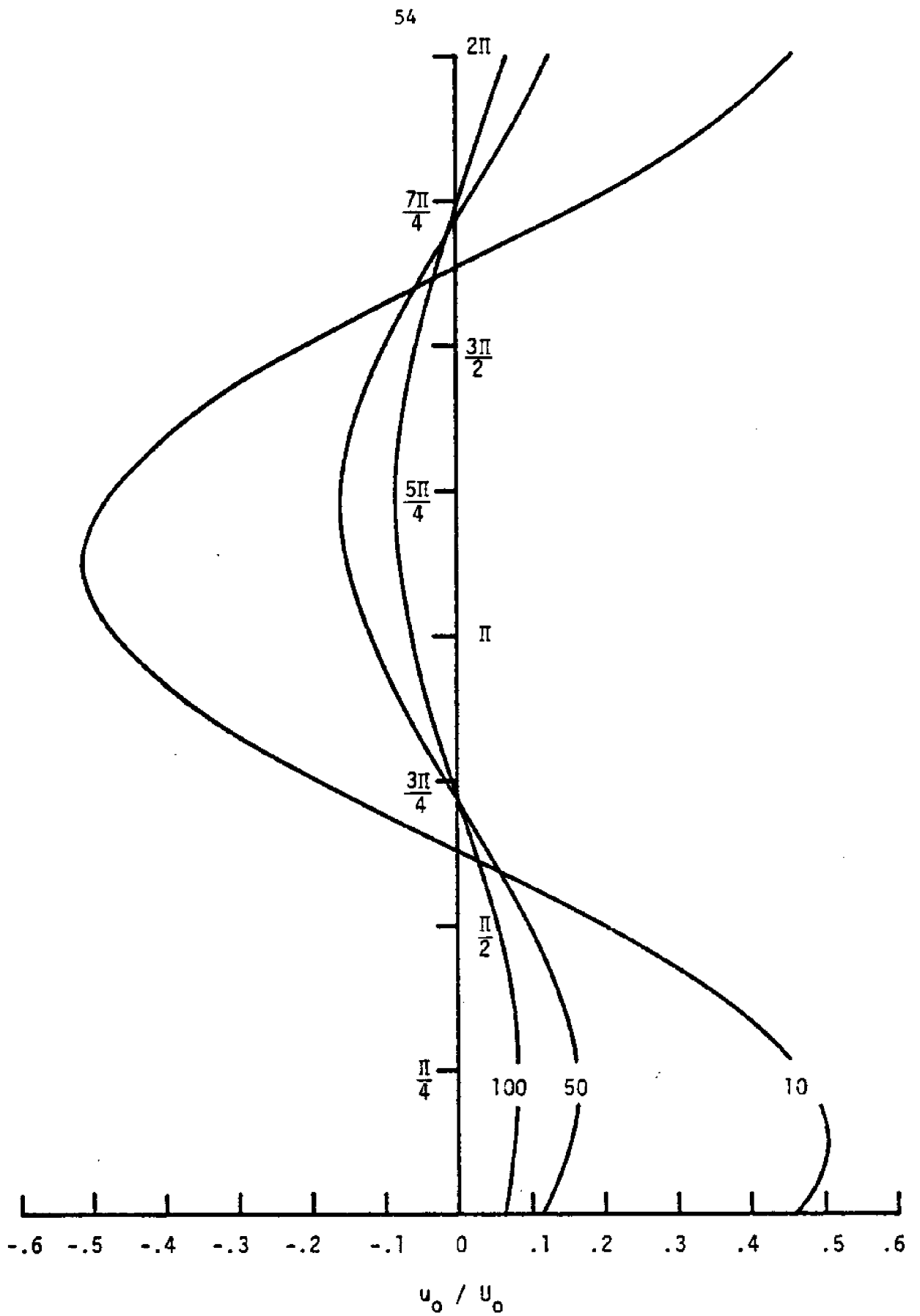$\delta \approx 0.5$ - 1.0 cm., as for boundary layer No.2 $\delta_2 \approx \sqrt{K} \leq 10^{-3}$ cm .

Thus this layer is so thin for ordinary porous beds that its thickness

is merely a fraction of the grain diameter. It has been noted by sev-

eral investigators (Murray, 1965) that the bed can become substantially

fluidized near the interface before significant motion occurs, i.e., the

bed reaches a "quick" state. If this is so, then the permeability will

be greatly increased and the layer will extend deeper into the bed,

thereby encompassing the first grain layer. This effect would decrease

the surface shear stress but increase the form drag of the interstitial

flow on the particles. The correction velocity in layer No.2 is

$$u_s' = \frac{a\sigma e^{z/\sqrt{K}}}{\sinh kd}(\cos\chi - \frac{\cos(\chi+\Theta^*)}{\xi} - \frac{\sigma K}{\nu}\cdot\sin\chi) \quad z \leq 0 \qquad (4.11)$$

Unlike its counterpart u', u_s' has no depth dependent phase. An ex-

ample of the velocity profile across boundary layer No.2 is shown in

Figure 4.6. Note that the negative scale is amplified in order to empha-

size the flow reversal within the bed.

4.5 Stream Functions

The stream function is defined by

$$u = -\psi_z \quad \text{and} \quad w = \psi_x . \qquad (4.12)$$

The stream function in both the major flow regions is modified near the

interface by a ψ' which corresponds to a u'. The stream function can be

found for the fluid domain by utilizing (3.11) and integrating (4.12).
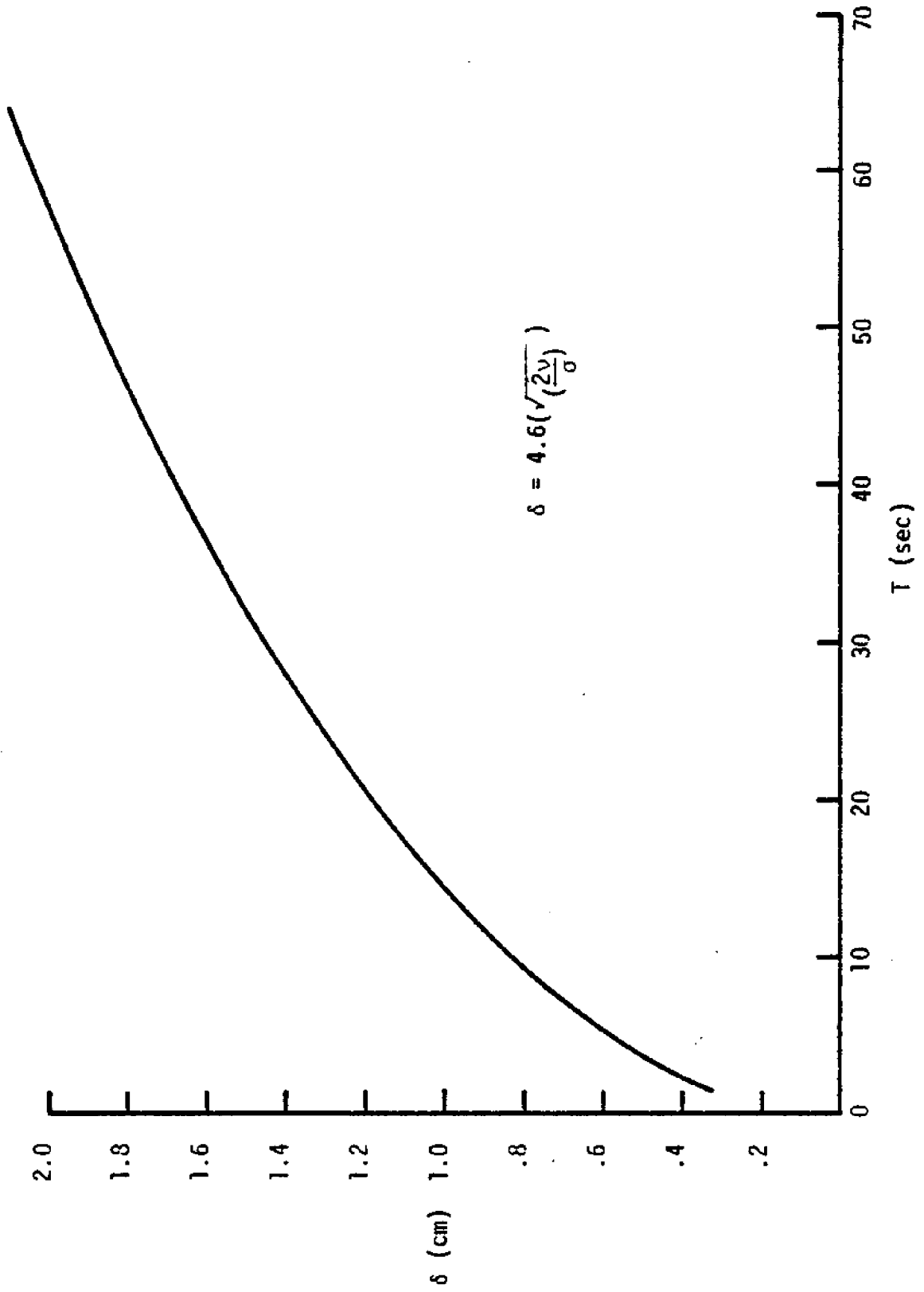
$$\delta = 4.6(\sqrt{\frac{2\nu}{\sigma}})$$
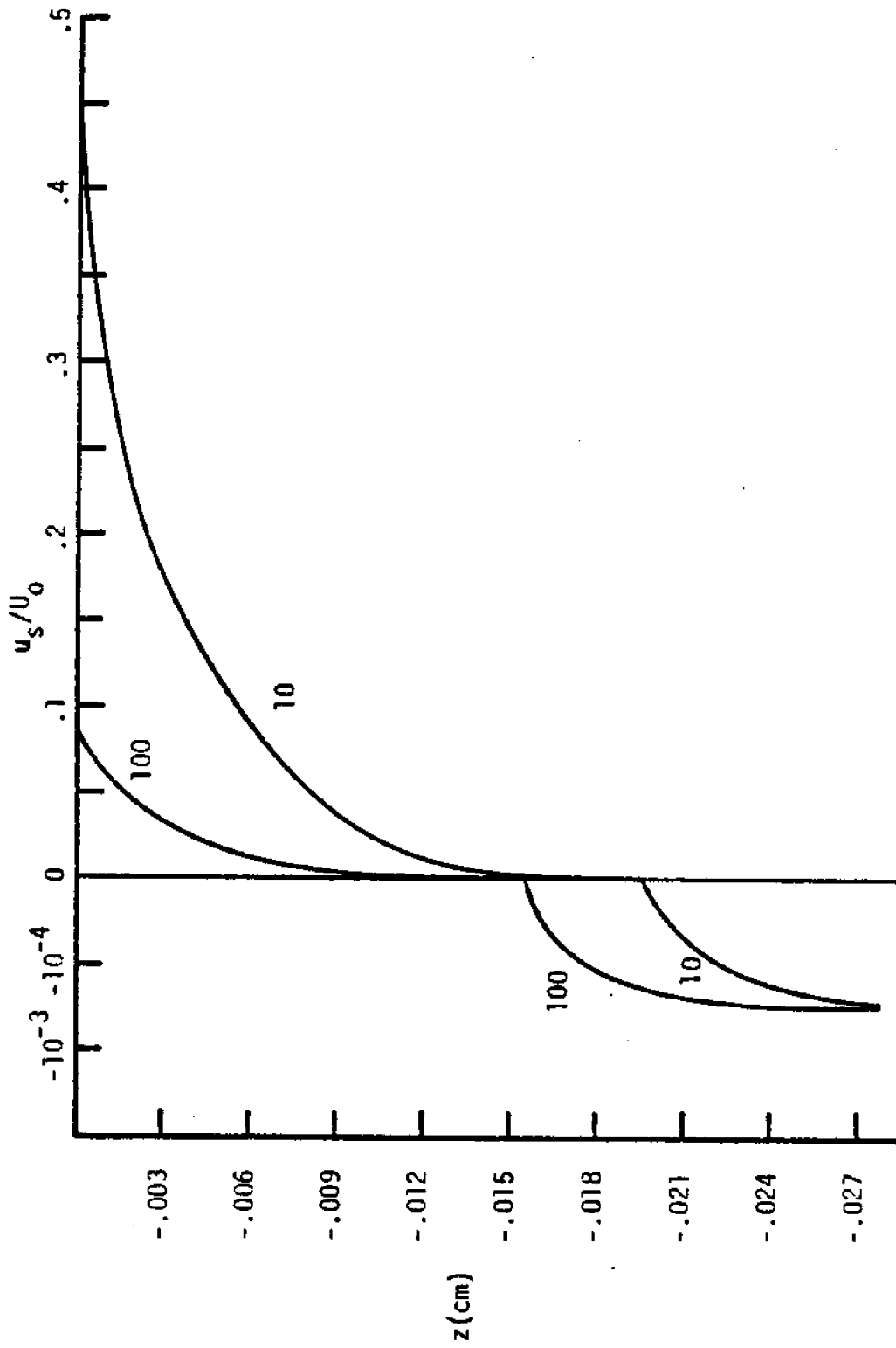
Figure 4.5   Boundary layer thickness vs wave period

Figure 4.6 u_s/U_o vs z , curves represent profiles for different values of $u/\sqrt{K}$ (cm^{-1}).
T = 8 sec , K = 10^{-5} cm^2, h = 7m, ν = .01 cm^2/sec

$$\psi = \frac{a\sigma}{\sinh kd} \left\{ -\frac{\sinh kz}{k} \cdot \cos\chi + \frac{(J^2+I^2)^{1/2}}{I} \left(\frac{\sigma\sqrt{K}\operatorname{sech}kh}{k\alpha\nu\xi} \right) \right.$$

$$\left. \cdot \cosh kz \cdot \cos\ (\chi+\Psi+\Theta^*) \right\} \ . \tag{4.13}$$

The second term represents a modification to the impermeable case. Its amplitude is small compared to the first term, except near the bottom where sinhkz approaches zero and coshkz approaches one. Under the approximations applied, the value of the second term depends on b , the parameter arising from the boundary layer solution and upon $\alpha/\sqrt{K}$, the parameter given in the boundary condition. It also has a phase advance of $\sim \pi/4$ and derives its existence from the pumping action in the bed. As can be seen in Figure 4.7, the streamlines in the bed intersect the interface.in advance of the external flow.

The stream function for the porous bed flow is

$$\tilde{\psi}_s = \frac{-a\sigma^2 K \sinh k(z+h)\cdot\sin\chi}{k\nu\sinh kd\cdot\cosh kh} \tag{4.14}$$

which is 90° in advance of the potential field stream function.

The approximate corrections to the stream functions in the boundary layers are given by

$$\psi^\prime = \frac{-a\sigma e^{-bz}\cdot\cos(\chi+bz+\Theta^*+\pi/4)}{\sqrt{2}\ \xi\ b\ \sinh kd} \tag{4.15}$$

and

$$\psi^\prime_s = \frac{-a\sigma\sqrt{K}\ e^{z/\sqrt{K}}}{\sinh kd} \left(\cos\chi - \frac{\cos(\chi+\Theta^*)}{\xi} - \frac{\sigma K}{\nu}\ \sin\chi \right) \ . \tag{4.16}$$
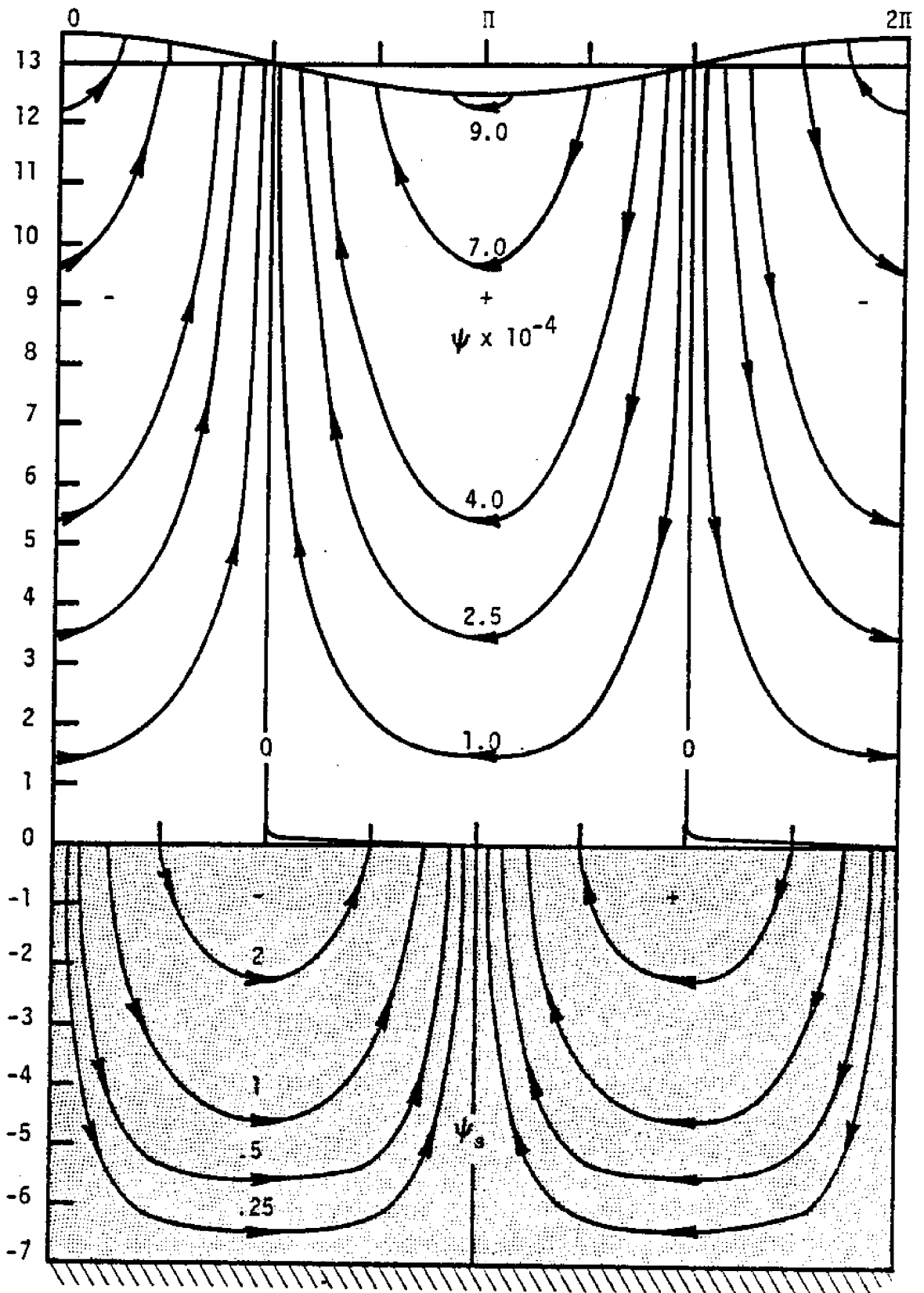
Figure 4.7   Streamlines   L = 100 m, d = 13 m,   h = 7 m, a = 1 m,
K = 10^{-6} cm^2, $\alpha/\sqrt{K}$ = 100/cm ν = .01 cm^2/sec

The last term in ψ_s^c is retained only because it is approximately 90° out of phase with the first two terms. The program called STREAMS found in Appendix 7.3 is used to calculate the stream function values in both the fluid and the bed for any size depth-increments and at phase increments of $\pi/8$.

4.6 Shear Stress

The shear stress at the interface is the main cause of sediment motion. Figure 4.8 shows the nondimensionalized shear stress with a representative number of measurements from Teleki and Anderson (1970). the quantity $\tau_o max/\rho$. $U_o U_o$ is proportional to the friction coefficient as stated in Equation (1.9). Unfortunately all of their data lies in what is considered to be the transition region ($35 < U_o\sqrt{2\nu/\sigma}/\nu < 910$). Also shown is the result from Kajiura's (1968) theory for C_f with $n = 0.5$. Teleki's data was collected using an impermeable sloping bottom (slope = 1:12.5). Nonetheless, the theoretical curve shows a correct trend across the transition zone. The laminar bottom shear stress is given by

$$\tau_o = \frac{\sqrt{2}\ \mu a \sigma b \cos(\chi + \Theta^* - \pi/4)}{\xi \sinh kd} \qquad (4.17)$$

The data points in Figure 4.8 are given in Appendix 7.1. The program DISSIP in Appendix 7.3 can be used to calculate both the dimensional and nondimensional forms of τ_o.

4.7 Energy Dissipation and Attenuation Coefficients

Energy dissipation occurs in all the regions. The values of d/L and h have the greatest affect on the relative importance on the energy
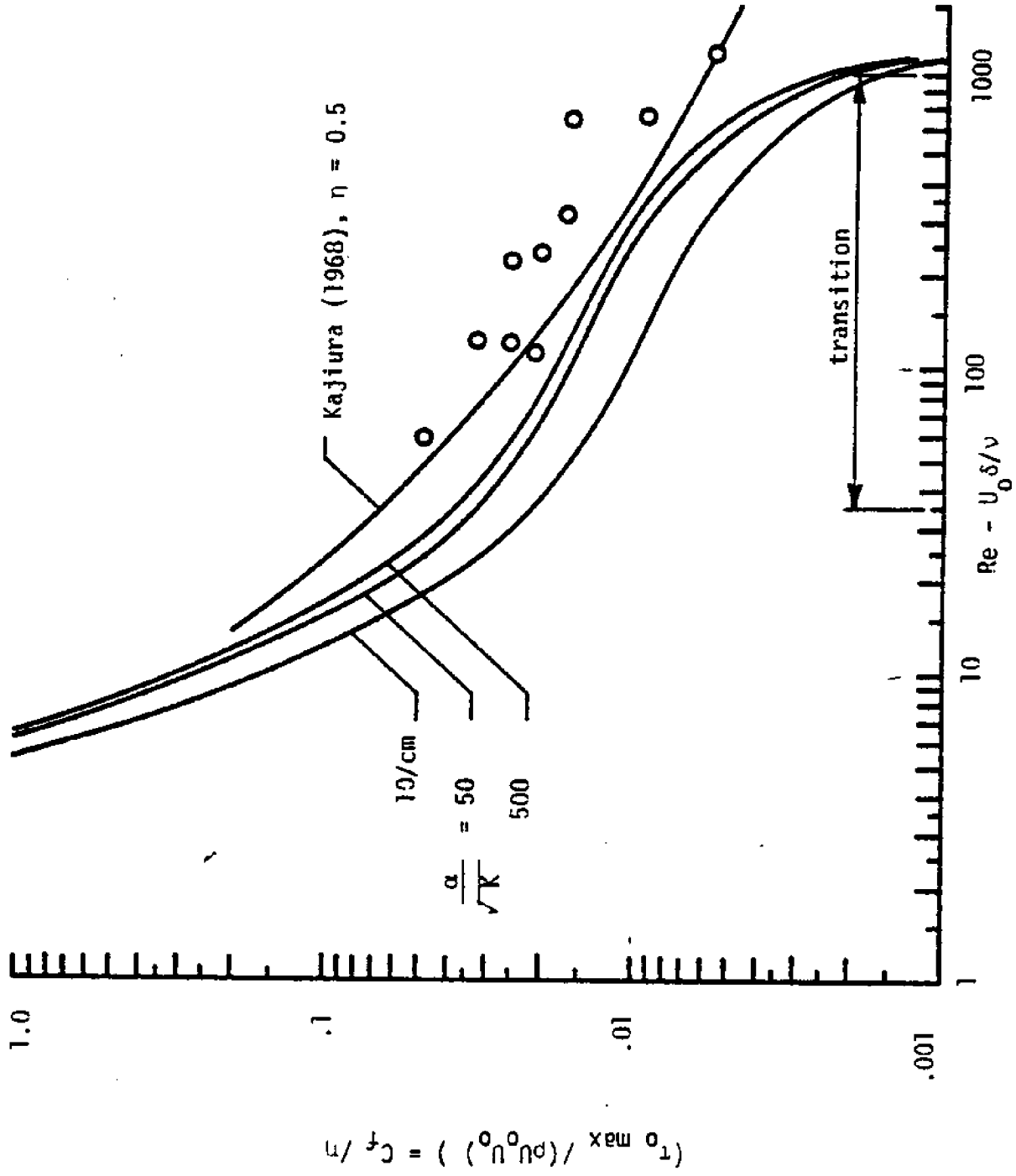
Figure 4.8 Comparison of nondimensionalized bottom shear and data from Teleki and Anderson (1970)

loss in the three major regimes. To calculate the rate of loss in the fluid region, Raleigh's dissipation function is employed (Rouse, 1938). Contributions will arise from the external flow and the boundary layer. Energy dissipation is given by

$$D = 2\mu \int_0^L \int_0^d [u_x^2 + w_z^2 + \frac{1}{2}(u_z + w_x)^2] \, dzdx \qquad (4.18)$$

where major contributors to fluid domain losses are given by

$$D = 4\mu \int_0^L \int_0^d [u_x^2 + w_z^2] \, dzdx + \mu \int_0^L \int_0^\infty (u_z')^2 \, dzdx \quad . \qquad (4.19)$$

The first term is due to the potential flow and the second is from the boundary layer. The first term is evaluated as

$$D_f = 4\pi\mu a^2 \sigma^2 \coth kd \; , \qquad (4.20)$$

an expression identical to Hough's (1896) result. The boundary layer loss is

$$D_{bl} = \frac{\mu b L}{2} \left(\frac{a\sigma}{\xi \cdot \sinh kd} \right)^2 \quad . \qquad (4.21)$$

The porous bed rate of loss is calculated in the same manner as Putnam's (1949) and Liu's (1973) determination, and is

$$D_{pb} = \frac{\mu}{K} \int_0^L \int_{-h}^0 (\tilde{u}_s^2 + \tilde{w}_s^2) \, dzdx = \frac{\rho K}{\pi\nu} \left(\frac{a\sigma^2 L}{2\sinh kd} \right)^2 \tanh kh \quad . \qquad (4.22)$$

This is exactly the same result as obtained by Reid and Kajiura (1957). Figures 4.9 and 4.10 show the relative contributions of D_{bl} and D_{pb} for a typical wavelength in various depths of water and over beds of various thicknesses. Figures 4.11 and 4.12 compare theoretical rates of energy loss to experimental values from Savage (1953). All of Savage's waves were intermediate waves and his data is given in Appendix 7.2.
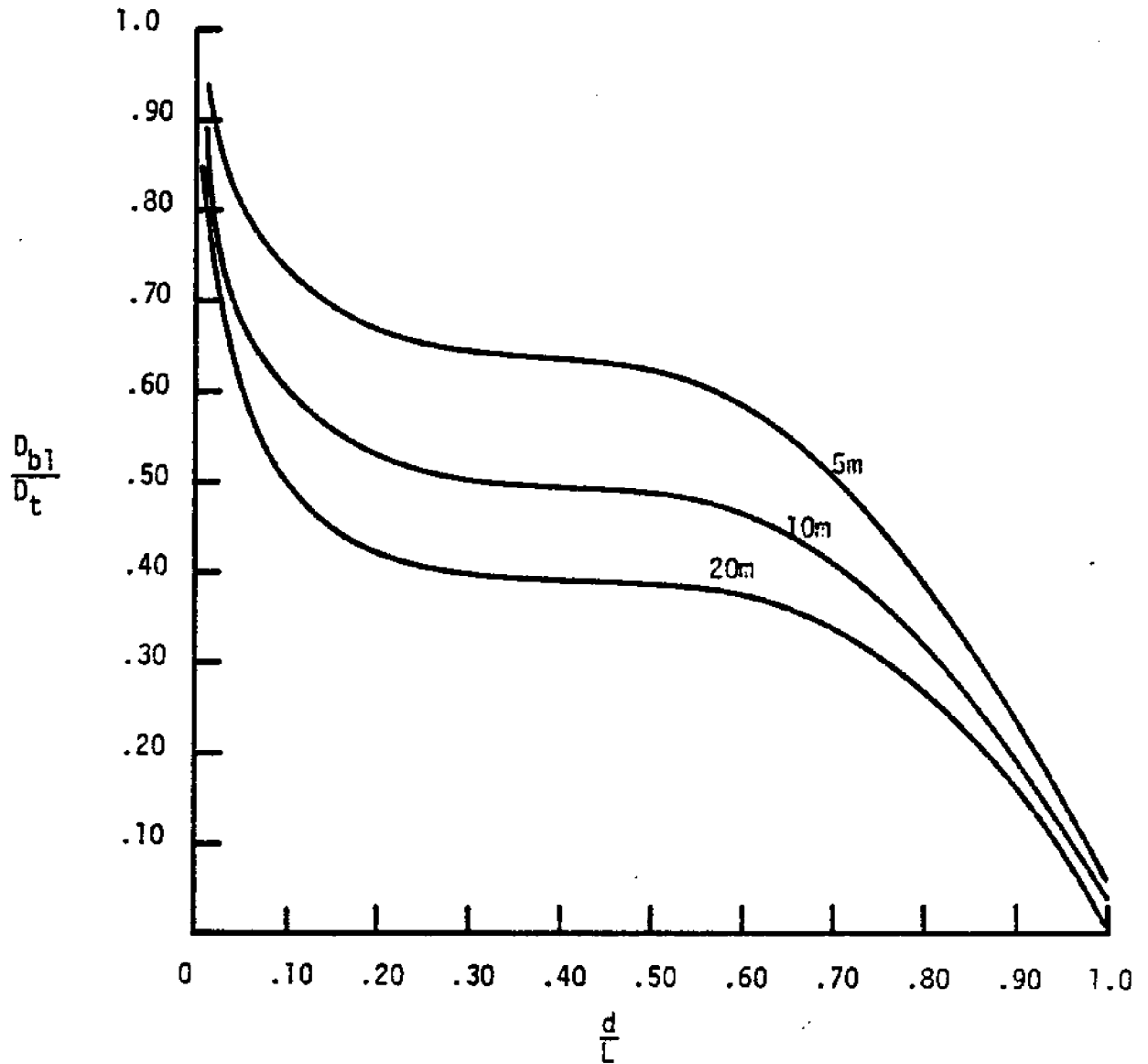
Figure 4.9   Fractional dissipation due to boundary layer vs
depth to wavelength ratio curves for various bed
thicknesses. $L = 100$ m., $K = 10^{-6}$ cm^2 ,
$\nu = .01$ cm^2/sec, $\alpha/\sqrt{K} = 100$ cm^{-1}
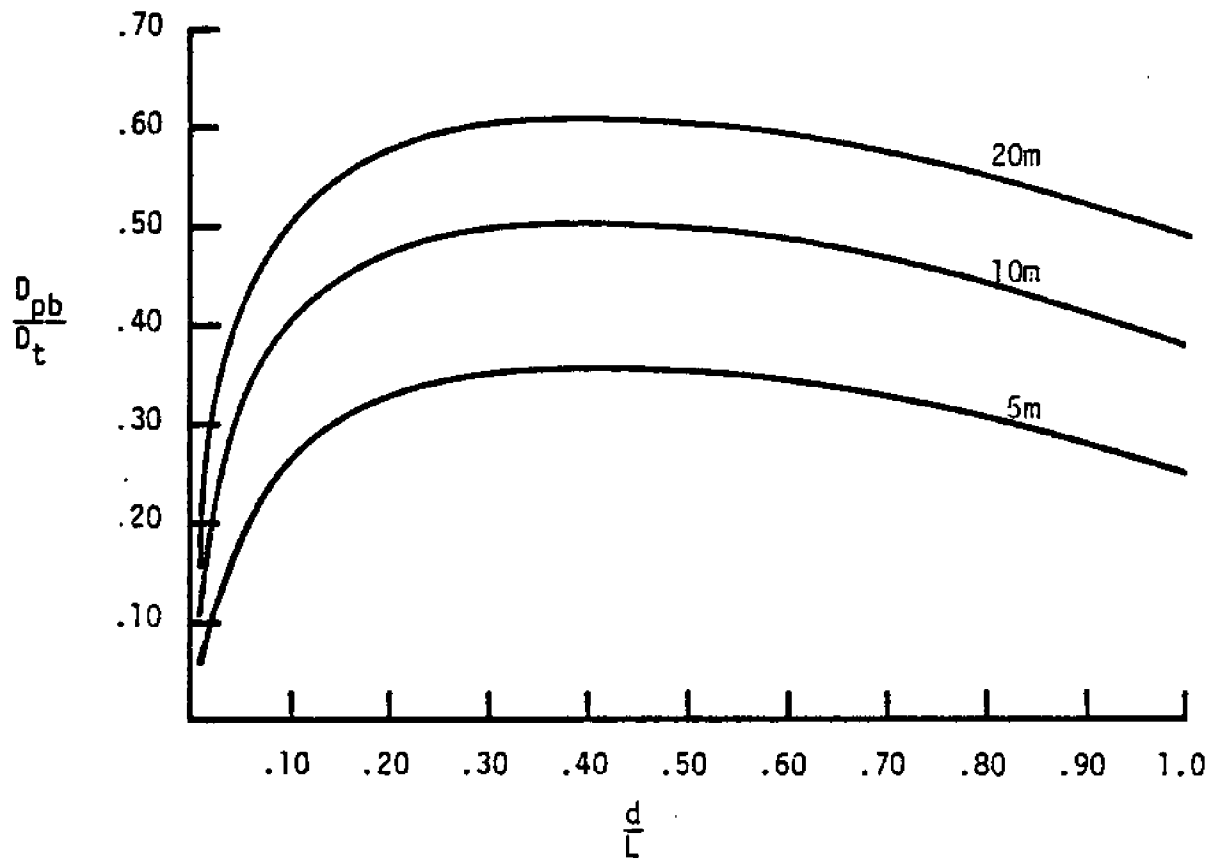
Figure 4.10 Ratio of porous bed dissipation to total energy
            loss. Curves for various bed depths   L = 100 m,
            $K = 10^{-6}$ cm^2 , $\alpha/\sqrt{K} = 100/$cm, $\nu = .01$ cm^2/sec
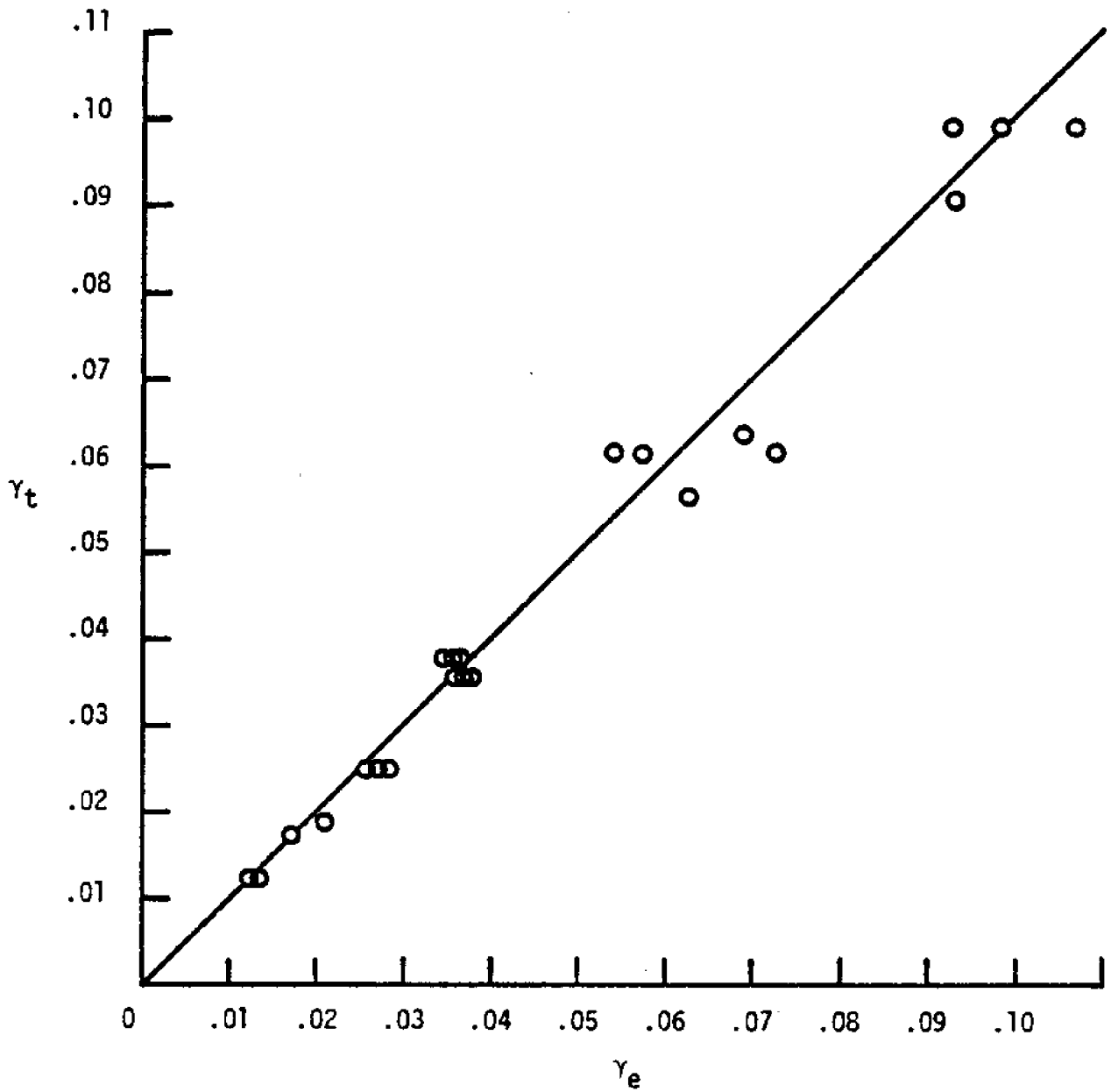
Figure 4.11 Comparison of theoretical and experimental attenuation coefficients; data by Savage (1953) $\nu = .01$ cm^2/sec, $\alpha/\sqrt{K} = 100$/cm
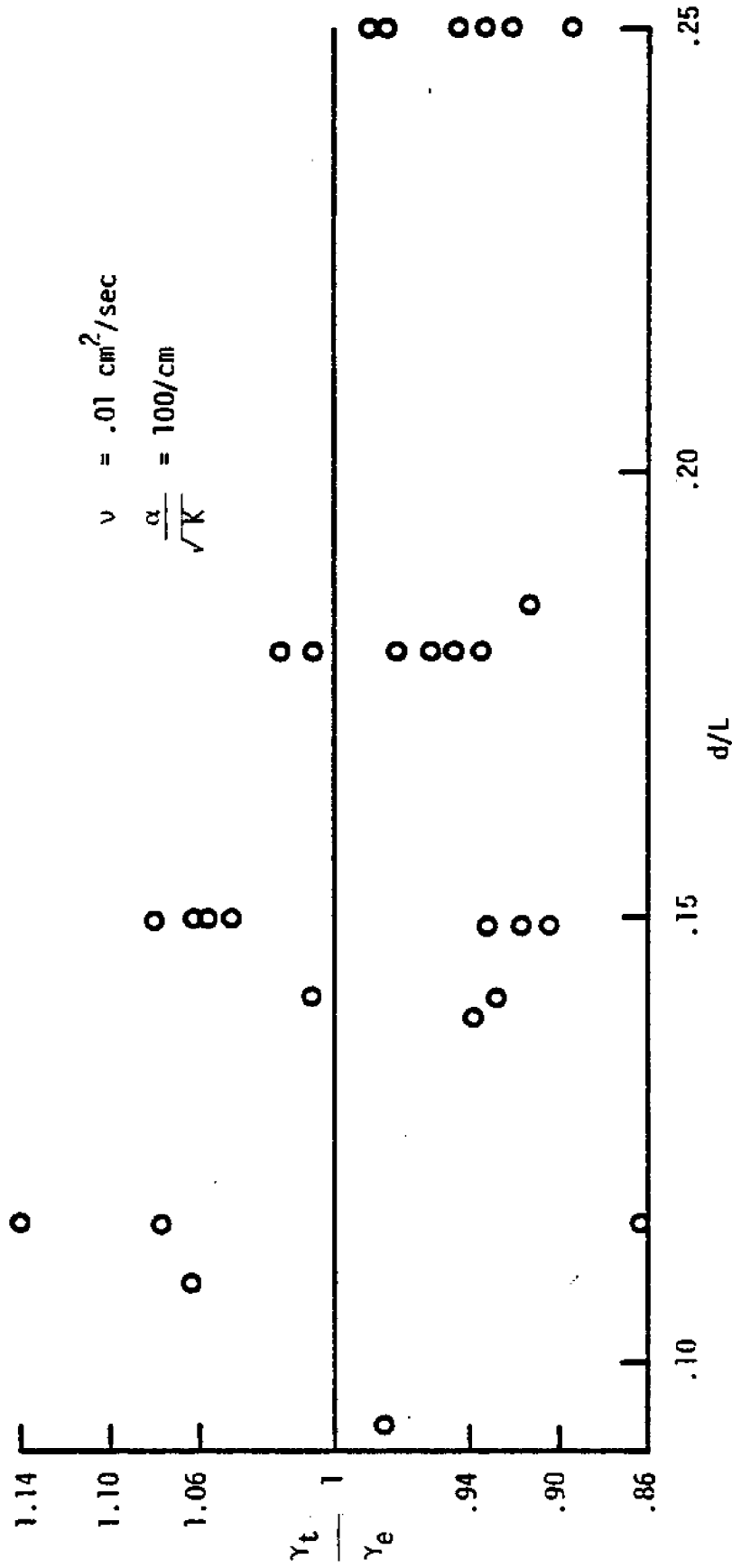
Figure 4.12 Comparison of theoretical to experimental attenuation coefficients vs depth/wave length. Data by Savage (1953)

The attenuation coefficient, γ , is defined as $D/2E$. The energy, E , of a small amplitude wave is $\rho g a^2 L/2$.

$-D = \dot{E} = \rho g a a_t L$ and $a_x = a_t/C_g$ where C_g is the group velocity and equals the rate of energy transmission in the wave, so

$$a_x = \frac{-2\gamma E}{\rho g a C_g L} = \frac{-\gamma a}{C_g} \ .$$

Therefore,

$$a = a_i e^{-\gamma x/C_g} = a_i e^{-\gamma t} \ . \tag{4.23}$$

It is found that the dispersive relationship obtained by satisfying the dynamic surface condition which was not utilized in section 3 does not change from the impermeable bed result under the simplifications made. The result is a definite relationship between σ and k in terms of the water depth.

$$\sigma^2 = gk\tank kd \ .$$

Therefore the phase speed is unaltered and the group velocity from Airy theory,

$$C_g = \frac{d\sigma}{dk} = \frac{1}{2} (\frac{g}{k} \cdot \tanh kd) \ (1 + \frac{2kd}{\sinh kd})$$

can be assumed.

This value of C_g was used in interpreting Savage's data. The program DISSIP was used to determine the energy losses for both Savage's data and the losses indicated in Figures 4.9 and 4.10. This program can be used for either discrete data or for systematically changing the values

of the wave, bed and boundary condition parameters. Substitution of certain cards can change the output from dimensional to nondimensional.

5 CONCLUSIONS

It has been shown that porous bed effects can produce significant adjustments in the structure of the bottom boundary layer. The results expressed here are subject to rather stringent restraints, i.e., that the bottom boundary layer is laminar and that the bed is stationary. Nonetheless, understanding of the laminar case is valuable to the understanding of the transition and turbulent flow regimes. Also, knowledge of the shear stress is a prerequisite to prediction of the threshold conditions. At present very little data exist on the boundary layer structure and the shear stress related to wave motion above a porous bed. Since the layer is typically very thin, measurements are difficult and new techniques need to be developed.

As for the radiation condition, for successful application to be accomplished, determination of α for natural bed materials is required. The properties of the bed at the interface may not be typical compared to the gross properties when pressure gradients and flow fields are present. If this is the case, the values of α, ϵ, and K will be altered. The question of whether sediment motion is a sudden event or is preceded by partial fluidization of the interface is a pertinent question. Once bed motion begins, the boundary condition becomes invalid and a new condition must be applied. A great deal of experimentation will be required to determine its form.

A direct extension of this paper is to determine mean lift and drag forces on individual particles. Exact calculation of these forces is possible since the flow pattern at the interface is known. Figure 5.1 shows a typical velocity profile and the lift and drag forces. The drag
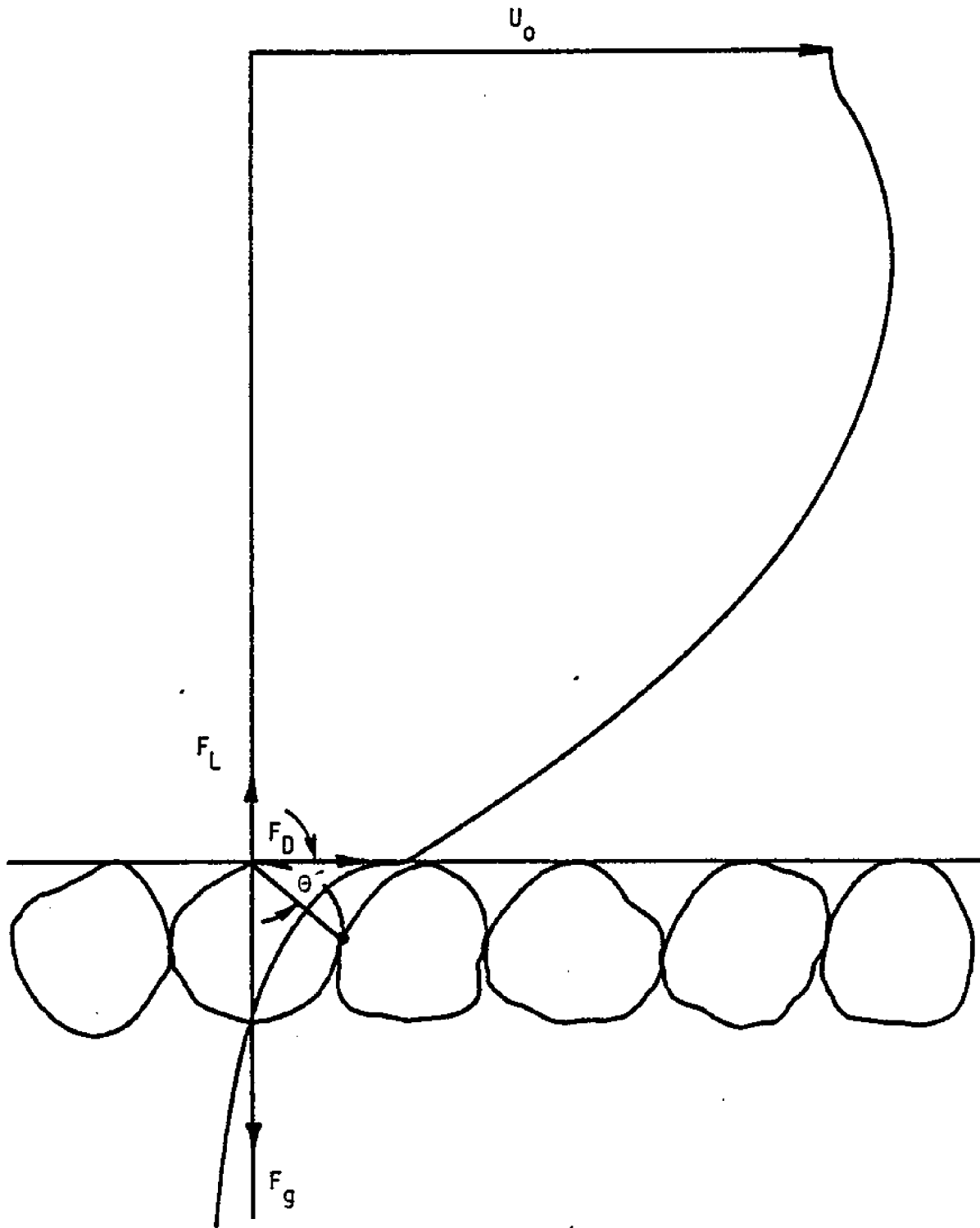
Figure 5.1 Forces acting on a sediment particle

force, F_D, contributes to the vertical force due to the moment about the contact point with the adjacent particle. The drag force is approximately equal to $\tau_0 \cdot (\pi D^2/4)$ where D is the sediment particle diameter. The lift force, F_L, approximately equal to $\rho u_s \Gamma = \rho u_s \int \int (u_s)_z dA$ where Γ is the circulation about the particle and A represents area. The lift and drag forces are opposed by the submerged weight of the particle, i.e., $F_g = -(\rho_s - \rho)g(\pi D^3/6)$. With these calculations, the threshold conditions can be approximated analytically. The author plans to continue this work and complete these calculations.

6 LIST OF REFERENCES

Bagnold, R. A. (1946) Motion of waves in shallow water, interaction between waves and sand bottoms. Proc. Roy. Soc., London, A 187: 1-15.

Batchelor, G. K. (1974) Transport properties of 2-phase materials with random structure. Annual Review of Fluid Mechanics 6:227-255.

Beavers, G. S., D. D. Joseph (1967) Boundary conditions at a naturally permeable wall. J. Fluid Mech., 30(1):197-207.

Boone, J. H. (1974) Current-wave interaction patterns near a tidal inlet. Unpublished master's thesis, North Carolina State University, Raleigh, N. C., 97 p.

Bretschneider, C. L. (1954) Field investigation of wave energy loss in shallow water ocean waves. Beach Erosion Board Tech. Memo. 46, 40 p.

Bretschneider, C. L., R. O. Reid (1954) Modification of wave height due to bottom friction, percolation and refraction. Beach Erosion Board Tech. Memo. 45, 36 p.

Brinkman, H. C. (1947) On the permeability of media consisting of closely packed porous particles. Appli. Sci. Res., A1:81-86.

Collins, J. I. (1963) Inception of turbulence at the bed under periodic gravity waves. J. Geophys. Res., 68(No.21):6007-6014.

Dalrymple, R. A. (1974) Discussion of "Damping of water waves over porous bed." ASCE, J. Hydr. Div. 100, HY 11:1725-1728.

Dean, R. G., P. S. Eagleson (1966) Finite amplitude waves, from Estuary and Coastline Hydrodynamics (A. T. Ippen, ed.) McGraw-Hill, N. Y. Chapter 2.

DeHaan, B. (1858) Tables D'Intergrales Definies. C. G. Van Der Post, Amsterdam, 572 p.

Eagleson, P. S. (1962) Laminar damping of oscillatory waves, ASCE, J. Hydr. Div. 88, HY 3:155-181.

Eagleson, P. S., R. G. Dean (1959) Wave-induced motion of bottom sediment particles. ASCE, J. Hydr. Div. 85, HY 10:53-79.

Einstein, H. A. (1972) A basic description of sediment transport on beaches, from Waves on Beaches and Resulting Sediment Transport (R. E. Meyer, ed.). Academic Press, N. Y., pp. 53-94.

Field, M. E., D. B. Duane (1972) Geomorphology and sediments of the Cape Kennedy inner continental shelf, U. S. Army C.E.R.C. Tech. Memo. Series.

Field, M. E., E. P. Meisburger, P. B. Duane (1971) Late pleistocene-holocene sedimentation history of Cape Kennedy inner continental shelf. 45th Annual Mtg. of the Soc. of Econ. Paleantologists and Mineralists, 337-338.

Grosch, C. E. (1962) Laminar boundary layer under a wave. Phys. of Fluids 5(No.10):1163-1167.

Grosch, C. E., S. J. Lukasik (1960) Viscous dissipation of shallow water waves. Phys. of Fluids 3(No.3):477-479.

Ho, R. T., L. W. Gelhar (1973) Turbulent flow with wavy permeable boundaries. J. Fluid Mech., 58(Pt.2):403-414.

Ho, R. T., L. W. Gelhar (1974) Interaction between turbulent flow and undular permeable boundaries. MIT Hydraulics Lab. Rep. 180.

Horikawa, K., A. Watanabe (1967) A study on sand movement due to wave action. Coastal Engng. in Japan 10:39-57.

Horikawa, K., A. Watanabe (1968) Laboratory study on oscillatory boundary layer flow. Coastal Engng. in Japan 11:13-28.

Hough, S. S. (1896) On the influence of viscosity on waves and currents. Proc. London Math. Soc., 1(V.28):264-288.

Huang, N. E. (1970) Mass transport induced by wave motion. J. Mar. Res. 28(No.1):35-50.

Hunt, J. N. (1959) On the damping of gravity waves propagated over a permeable surface. J. Geophys. Res., 64(4):437-442.

Iwagaki, Y., Y. Tsuchiya, H. Chen (1967) On the mechanism of laminar damping of oscillatory waves due to bottom friction. Bull. Disast. Prev. Res. Inst., Kyoto U. 16(3)No.116:49-75.

Iwagaki, Y., Y. Tsuchiya, M. Sakai (1965) Basic studies on the wave damping due to bottom friction. Coastal Engng. in Japan 8:37-49.

Jain, S. C., J. F. Kennedy (1974) Spectral evolution of sedimentary bed forms. J. Fluid Mech., 63(Pt.2):301-314.

Jonsson, I. G. (1965) Measurements in the turbulent wave boundary layer. Proc. IAHR Congress, London, 85-92.

Jonsson, I. G. (1966) Wave boundary layers and friction factors. Proc. 12th Conf. Coastal Engng. 127-148.

Kajiura, K. (1964) On the bottom friction in an oscillatory current. Bull. Earthquake Res. Inst., 42:147-174.

Kajiura, K. (1968) A model of the bottom boundary layer in water waves. Bull. Earthquake Res. Inst., 46:75-123.

Kalkanis, G. (1957) Turbulent flow near an oscillatory wall. Beach Erosion Board Tech. Memo. 97, 36 p.

Keulegan, G. H. (1950) Wave motion, from Engineering Hydraulics (H. Rouse, ed.) John Wiley and Sons, N. Y., Chapt. 11.

Keulegan, G. H., G. W. Patterson (1940) Mathematical theory of irrotational translation waves. R. P. 1272, J. Res. Nat. Bur. Std. 24, 47 p.

Komar, P. D., M. C. Miller (1974) Sediment threshold under oscillatory waves. Proc. Conf. Coastal Engng. Vol. 1, Pt. 1:757:775.

Komar, P. D., R. H. Neudeck, L. D. Kulm (1972) Observations and significance of deep-water oscillatory ripple marks on the Oregon continental shelf, from Shelf Sediment Transport (Swift, Duane, Pilkey, eds.) Dowden, Hutchinson and Ross, Stroudsburg, Pa., Chapt. 25.

Laitone, E. V. (1962) Limiting conditions for cnoidal and Stokes waves. J. Geophys. Res., 67:1555-1564.

LeMehauté, B., D. Divoky, A. Lin (1968) Shallow water waves: a comparison of theories and experiments. Proc. Conf. Coastal Engng. Pt. 1:86-107.

Li, H. (1954) Stability of oscillatory laminar flow along a wall. Beach Erosion Board Tech. Memo. 47, 48 p.

Lighthill, M. (1963) Introduction, real and ideal fluids, from Laminar Boundary Layers, (L. Rosenhead, ed.) Oxford Uni. Press, London, Chapt. 1.

Liu, P., (1973) Damping of water waves over porous bed. ASCE, J. Hydr. Div. 99, HY 12:2263-2271.

Lonquet-Higgins, M. S. (1958) The mechanics of the boundary layer near the bottom of a progressive wave. Proc. Conf. Coastal Engng. 184-193.

Lukasik, S. J., C. E. Grosch (1963) Discussion of "Laminar Damping of Oscillatory Waves." ASCE, J. Hydro. Div. 89, HY 1:232:239.

Manohar, M. (1955) Mechanics of bottom sediment movement due to wave action. Beach Erosion Board Tech. Memo., 75, 121 p.

Masch, F. D. (1961) Cnoidal Waves: Tables of Functions, Council on Wave Research, Richmond, Calif.

McQuivey, R. S. (1973) Summary of turbulence data from rivers, conveyance channels, and laboratory flumes. U. S. Geological Sur. Prof. Paper 802-B, 66 p.

Millikan, J. D., O. H. Pilkey, D. A. Ross (1972) Sediments of the continental margin off the eastern U.S., Geo. Soc. Am. Bull., 83(No.5):1315-1333.

Murray, J. D. (1965) Viscous damping of gravity waves over a permeable bed. J. Geophys. Res., 70(No.10):2325-2331.

Peregrine, D. H. (1972) Equations for water waves and the approximations behind them, from Waves on Beaches and Resulting Sediment Transport (R. E. Meyer, ed.) Academic Press, N. Y., Chapt. 3.

Phillips, O. M. (1969) The Dynamics of the Upper Ocean. Cambridge University Press, Cambridge, 261 p.

Pilkey, O. H., M. E. Field (1972) Onshore transportation of continental shelf sediment: Atlantic Southeastern U. S., from Shelf Sediment Transport (Swift, Pilkey, Duane, eds.) Dowden, Hutchinson, and Ross, Stroudsburg, Pa., Chapt. 21.

Putnam, J. A. (1949) Loss of wave energy due to percolation in a permeable sea bottom. Trans. Am. Geophys. Union 30(No.3):349-356.

Putnam, J. A., J. W. Johnson (1949) The dissapation of wave energy by bottom friction. Trans. Am. Geophys. Union 30(No.1):67-74.

Radwan, A. M., N. E. Huang, C. C. Tung (1975) Wave-current interactions in water of variable depth. Center for Mar. and Coastal Studies-NCSU Rep. 75-3, 30 p.

Rance, P. J., N. F. Warren (1968) The threshold of movement of coarse material in oscillatory flow. Proc. Conf. Coastal Engng. Pt. 1: 487-491.

Reid, R. O., K. Kajiura (1957) On the damping of gravity waves over a permeable sea bed. Trans. Am. Geophys. Union 38(No.5):662-666.

Reidel, H. P., J. W. Kamphuis, A. Brebner (1972) Measurement of shear stress under waves. Proc. Conf. Coastal Engng. Pt.1:587-604.

Richardson, S. (1971) A model for the boundary condition of a porous material. Part 2. J. Fluid Mech., 49(Pt.2):327-336.

Rouse, H. (1961) Fluid Mechanics for Hydraulic Engineers. Dover Publ., N. Y. 442 p.

Saffman, P. G. (1971) On the boundary condition at the surface of a porous medium. Studies Appl. Math., 1(No.2):93-101.

Savage, R. P. (1953) Laboratory study of wave energy losses by bottom friction and percolation. Beach Erosion Board Tech. Memo. 31, 28p.

Schlichting, H. (1968) Boundary Layer Theory. McGraw-Hill, N.Y. 748 p.

Skjelbreia, L. (1959) Gravity Waves, Strokes Third Order Approximation, Table of Functions. Published by the Council on Wave Research, The Engineering Foundation, Univ. of Calif., Berkeley, Calif.

Sleath, J. F. A. (1968) The effect of waves on the pressure in a bed of sand in a water channel and on the velocity distribution above it. Unpublished Ph.D thesis, St. John's College, Cambridge, 141 p.

Sleath, J. F. A. (1970) Wave-induced pressures in beds of sand. ASCE, J. Hydr. Div. 96, HY 2:367-378.

Taylor, G. I. (1971) A model for the boundary condition of a porous material. Part 1. J. Fluid Mech., 49(Pt.2):319-326.

Teleki, P. G. (1972) Velocity and shear stress in wave boundary layers. Proc. Conf. Coastal Engng. Pt. 1:569-586.

Teleki, P. G. (1972) Wave boundary layers and their relation to sediment transport, from Shelf Sediment Transport (Swift, Duane, Pilkey, eds.) Dowden, Hutchinson and Ross, Stroudsburg, Pa., Chapt. 2.

Teleki, P. G., M. W. Anderson (1970) Bottom boundary shear stresses on a model beach. Proc. Conf. Coastal Engng., Pt. 1:269-288.

Treloar, P. D., A. Brebner (1974) Energy losses under wave action. Proc. Conf. Coastal Engng., Pt. 1:257-267.

Tunstall, E. B., D. L. Inman (1975) Vortex generation by oscillatory flow over rippled surfaces. J. Geophys. Res. 80(No.24):3475-3484.

Vincent, G. E. (1957) Contribution to the study of sediment transport on a horizontal bed due to wave action. Proc. Conf. Coastal Engng., 326-355.

Yalin, M. S. (1972) Mechanics of Sediment Transport. Pergamon
      Press, N. Y., 290 p.

Zaslavskii, D. I., S. Irmay, J. Bear (1968) Physical Principles of
      Water Percolation and Seepage. U.N.E.S.C.O., Paris, 465.

7 APPENDICES

Appendix 7.1

Derivation of Φ_c

As described in section 2.3, the determination of Φ facilitates the evaluation of α . In order to clarify the implications of assuming a constant velocity shear across the fluid-bed interface, the quantity Φ_c was added on to the Figures 2.1 and 2.2.

Poiseuille flow:

$$u_{zz} = \frac{1}{\mu} P_x = 2F \qquad\qquad x \geq 0$$

Solution:

$$u = Fz^2 + Az + B$$

Porous bed flow:

$$(u_s)_{zz} - \frac{1}{K} u_s = 2F \qquad\qquad z \leq 0$$

Solution:

$$u_s = Ce^{z/\sqrt{K}} + De^{-z/\sqrt{K}} - 2\,KF$$

The solid boundary of the Poiseuille flow is located at $z = d$ and the bed is considered to be infinitely deep. The boundary conditions are

1. $u = 0$ at $z = d$.
2. $u_z = (u_s)_z$ at $z = 0$.
3. $u = u_s$ at $z = 0$.
4. u_s is bounded as $|z|$ increases.

The values of the constants are evaluated as

$$A = \frac{F(2-\zeta^2)\sqrt{K}}{(1 + \zeta)}$$

$$B = - \frac{Fd \sqrt{K}\ (2+\zeta)}{(1+\zeta)}$$

$$C = \frac{F(2-\zeta^2)K}{(1+\zeta)}$$

$$D = 0$$

where $\zeta = d/\sqrt{K}$. The values of Q and Q_i can be determined by integrating u from $z = 0$ to $z = d$.

$$Q_i = - F\left(\frac{d^3}{6}\right) , \qquad Q = - F\left(\frac{2d^3}{3} + \frac{\sqrt{K}d^2 (2-\zeta^2)}{2(1+\zeta)}\right) .$$

Finally,

$$\phi_c = \frac{Q - Q_i}{Q_i} = 3\left(\frac{\zeta+2}{\zeta(\zeta+1)}\right).$$

Appendix 7.2

Data

Orders of magnitude for physical parameters

Parameter	Definition	Value
L	Wavelength	$\geq 10^3$ cm
T	Period	$> 10^0$ sec
ν	Kinematic viscosity	10^{-2} cm^2/sec
ρ	Density	10^0 gr/cm^3
μ	Dynamic viscosity	10^{-2} gr/cm·sec
k	Wave number	$< 10^{-2}$ /cm
σ	Frequency	$\leq 10^0$ /sec
b		$\leq 10^1$ /cm
K	Permeability	$\leq 10^{-5}$ cm^2
ϵ	Porosity	0.5
α		$10^{-1} - 10^1$
$\alpha / \sqrt{K}$		$10^1 - 10^2$ /cm
θ		$\geq 3 \cdot 10^2$ /cm
λ		$\leq 10^{-8}$ cm
$\hat{\epsilon}$	Expansion parameter	≤ 0.10

Data from Teleki and Anderson (1970)

Re	$\tau_0/ (\rho U_0^2)$
60	.048
112	.021
122	.025
124	.034
224	.025
238	.020
322	.017
666	.009
1060	.006

Data from Savage (1953)

Run	d(cm)	$K \cdot 10^5 (cm^2)$	L(cm)	$\ln(H_o/H_f)$	γ
29	10.3	4.47	71.3	2.49	.098
28			71.3	2.71	.107
27			93.0	2.09	.093
26			109.7	1.99	.093
25	15.2		83.2	1.51	.062
24			109.7	1.39	.068
22			131.1	1.08	.057
23			131.1	1.37	.073
21			131.1	1.02	.054
20	22.8		92.0	.64	.026
11				.65	.026
10				.68	.027
19				.68	.027
9				.67	.027
18				.70	.028
17			124	.73	.037
8				.73	.037
7				.72	.036
6				.72	.036
15				.75	.038
5				.74	.037
4			154	.61	.035
14				.63	.036
2				.62	.036
13				.62	.036
3				.60	.035
12				.62	.036
1				.62	.036
77		2.14	91.4	.31	.013
78			91.4	.33	.013
76			126.8	.34	.017
75			126.8	.35	.018
73			153.6	.36	.021
72			153.6	.36	.021
74			153.6	.35	.020

Length of tank test section, 1829 cm

Appendix 7.3

Computer Programs

```
C PROGRAM TO CALCULATE BOUNDARY LAYER PROFILES OVER A POROUS BED
C UBL1=HORIZONTAL VELOCITY/MAX EXTERNAL VEL, UO(MAX)
C APM=BOUNDARY PARAMETER, PROPORTIONAL TO 1/SQRT(PM), PM=PERMEABILITY
C T=PERIOD, Z=VERTICAL DISTANCE FROM INTERFACE
C M,M6,M7= # OF VALUES OF T,APM,AND Z RESPECTIVELY
C Z1=RELATIVE VERTICAL DISTANCE FROM INTERFACE WRT B.L. THICKNESS
      DIMENSION UBL1(10),AAPM(5)
      M=6
      M6=4
      M7=9
      PI=3.141593
      V=0.01
   10 FORMAT(4F10.2)
      READ(1,10) (AAPM(J),J=1,M6)
    2 FORMAT(/,3X,'APM',9X,'0',8X,'22,5',8X,'67.5',8X,'90',7X,'1
     212.5',7X,'135',7X,'157.5',7X,'180 DEGREES')
      WRITE(3,2)
C DO LOOP FOR T
      DO 2000 I=1,M
      T=2**I
      WN=2.0*PI/T
      B=SQRT(WN/(2.0*V))
      BLT=4.6/B
C DO LOOP FOR Z1
      DO 1000 L=1,M7
      Z1=(M7-L)*4.6/(M7-1.0)
   20 FORMAT(///,3X,'T=',F6.1,3X,'V=',F5.3,3X,'BLT=',E9.2,3X,'Z1=',E9.2)
      WRITE(3,20) T,V,BLT,Z1
C DO LOOP FOR APM
      DO 1000 J=1,M6
      APM=AAPM(J)
C DO LOOP FOR PHASE ANGLE AND UBL1
      DO 900 K=1,9
      K1=K-1
      ARG1=K1*PI/8.0
      ARG2=ARG1+ATAN(B/(B+APM))+ Z1
      H=(1.0+2.0*B/APM+2.0*(B/APM)**2)
      UBL1(K)=COS(ARG1)-COS(ARG2)/(SQRT(H)*EXP(Z1))
  900 CONTINUE
   50 FORMAT(F8.2,9E11.2)
      WRITE(3,50) APM,(UBL1(N),N=1,9)
 1000 CONTINUE
   60 FORMAT(//////)
      WRITE (3,60)
 2000 CONTINUE
      CALL EXIT
      STOP
      END
```

```
C CALCULATION OF DISSIPATION RATE/UNIT WIDTH OF WAVE ENERGY, ATTENUA-
C TION CONSTANT AND MAX BOTTOM SHEAR STRESS-CONSTANT WATER AND BED
C DEPTH AND THICKNESS
C VARIABLES-WL,A,D,H,PM, C =CONST/SQRT(PM)--DISCRETE DATA-DIMENSIONAL
C DF=DISSIP RATE IN FLUID REGIME
C DBL= " " IN BOUNDARY LAYER
C DPB= " " IN POROUS BED
C DT= TOTAL DISSIP RATE
C SSO= BOTTOM SHEAR STRESS
C ATC=ATTENUATION CONSTANT
C WL=WAVELENGTH,A=AMPLITUDE,D=DEPTH,H=BED THICKNESS,PM=PERMEABILITY
C T=PERIOD OF WAVE
C DFI,DBLI,DTI,SSOI,TI=QUANTITIES FOR IMPERMEABLE CASE
C C=SURFACE PARAMETER,DV=DYN VISCOSITY, G=GRAV ACC,DN=DENSITY
C INVERSE OF BI AND B IS THE BOUNDARY LAYER THICKNESS,
C UO=POTENTIAL VELOCITY AT THE BOTTOM
C RE=WAVE REYNOLDS NUMBER
C CG=GROUP VELOCITY
C CP=PHASE VELOCITY
      1 DIMENSION WLA(20),AA(20),DA(10),HA(10),PMA(5),CA(5)
        CTNH(WD)=COSH(WD)/SD
        PI=3.14
      2 FORMAT(3F8.3)
      3 READ(1,2)DV,DN,G
      4 FORMAT('DV=',F4.3,5X,'DN=',F5.3,5X,'G=',F5.1,//)
        WRITE(3,4)DV,DN,G
C READ IN THE NUMBER OF COMPONENTS OF EACH ARRAY
      5 FORMAT(6I8)
        READ(1,5)M1,M2,M3,M4,M5,M6
        V=DV/DN
C READ IN DATA ARRAYS
      6 FORMAT(8F10.2)
        READ(1,6)(WLA(I),I=1,M1),(AA(J),J=1,M2),(DA(K),K=1,M3),(HA(L),L=1,
       2M4),(CA(N),N=1,M6)
     22 FORMAT(3F20.8)
        READ(1,22)(PMA(M),M=1,M5)
C DO LOOP FOR WL
      7 DO 2000 I=1,M1
        WL=WLA(I)
        WN=2*PI/WL
C AMPLITUDES HAVE 1-1 CORRESP. WITH WL, THEREFORE NO DO LOOP FOR A, SET
        J=I
        A=AA(J)
        AWN=A*WN
C NESTED DO LOOP FOR D
      8 DO 2000 K=1,M3
        D=DA(K)
        AD=A/D
C NESTED DO LOOP FOR H
      9 DO 3000 L=1,M4
        H=HA(L)
```

```
C NESTED DO LOOP FOR PM
   10 DO 3000 M=1,M5
      PM=PMA(M)
C NESTED DO LOOP FOR C WHICH IS PROPORTIONAL TO 1/SQRT(PM)
   11 DO 3000 N=1,M6
      C=CA(N)
      WD=WN*D
      WH=WN*H
      SD=SINH(WD)
      CH=COSH(WH)
      TD=TANH(WD)
C CALCULATE UNKNOWNS FOR IMPERMEABLE CASE, TI,SSOI,DFI,DBLI,DTI,ATCI
C ONLY DO THIS WHEN D CHANGES, SO
      IF(L*N*M .GT. 1) GO TO 25
      TI=SQRT(2.0*PI*WL*CTNH(WN*D)/G)
      FI=2*PI/TI
      BI=SQRT(FI/(2.0*V))
      DFI=-2*PI*DV*(A*FI)**2*CTNH(WN*D)
      DBLI=-DV*BI*WL*(A*FI/(2*SD))**2*2
C DTI=TOTAL DISSIP
      DTI=DFI+DBLI
      UO=A*FI/SD
      RE=UO*4.6/(BI*V)
C E=TOTAL MECHANICAL ENERGY PER UNIT WIDTH
      E=DN*G*WL*A**2/2.0
      ATCI= DTI/(2*E)
      SSOI=BI*DV*A*FI*SQRT(2.0)/SD
      AFI2=DFI/FTI
      ABLI2=DBLI/DTI
      SSOI2=SSOI/(DN*UO*UO)
   12 FORMAT(///,2X,'WL=',E10.3,2X,'A=',E10.3,2X,'D=',E10.3,2X,'BI=',E10
     2.3,2X,'AWN=',E10.3,2X,'AD=',E10.3,2X,'UO=',E10.3,2X,'RE=',E10.3)
      WRITE(3,12) WL,A,D,BI,AWN,AD,UO,RE
   19 FORMAT(1X,'IMPERMEABLE CASE',10X,'TI=',8X,'SSOI=',6X,'DFI=',7X,'DB
     2LI=',6X,'DTI=',7X,'ATI=')
      WRITE(3,19)
   20 FORMAT(25X,E9.3,5E11.3)
      WRITE(3,20)TI,SSOI,DFI,DBLI,DTI,ATCI
   30 FORMAT(/,2X,'PERMEABLE CASE')
      WRITE(3,30)
   21 FORMAT(2X,'H=',6X,'PM=',8X,'C=',5X,'T=',9X,'SSO=',7X,'DF=',8X,'DBL
     2=',7X,'DPB=',7X,'DT=',8X,'ATC=',8X,'CG=',8X,'CP=')
      WRITE(3,21)
C CALCULATE UNKNOWNS T,SSO,DBL,DF,DPB,DT,ATC,FOR PERMEABLE CASE
C SINCE THE EQN FOR T IS NONLINEAR AND TRANSCENDENTAL EVEN WHEN
C C>>B, TI WILL BE USED IN THE CALCULATION OF B IN THE EXPRESSION FOR T
   25 C1=C*C+2.0*BI*C+2.0*BI*BI
```

```
      C2=C*C*(WN/BI)**2/2+TD*TD-WN*TC/BI)+2.0*(BI*TD)**2+2.0*BI*TD*TD*C
      C3=(WN*C-2.0*(C*BI+BI*BI)*TD)/(WN*C+2.0*BI*BI*TD)
      C4=(WN*C*TD-2.0*(C*BI+BI*BI))/(2.0*BI*BI+WN*C*TD)
      ARGD=ATAN(C3)-ATAN(C4)
      T=SQRT(2*PI*WL/G*SQRT(C1/C2))*COS(ARGD/2)
      F=2*PI/T
      B=SQRT(F/(2*V))
      Q1=2*A*F*C*WN*B*DV/SD
      Y1=2.0*WN*(C+B)
      Z1=-2*WN*B
      SSO=Q1*SQRT(2.0/(Y1**2+Z1**2))
      SSO2=SSO/(DN*UO*UO)
      DF=DFI
      DBL=-DV*B*WL*(A*F/SD)**2/(4*(1+2*B/C+2*(B/C)**2))*2
      DPB=-(2*PI*WL*A/(T*T*SD))**2*PI*PM*DN/V*TANH(WN*H)
      DT=DF+DBL+DPB
      ATC=DT/(2.0*E)
      AF2=DF/DT
      ABL2=DBL/DT
      APB2=DPB/DT
      CP=WL/T
      CG=CP*(1.0+2.0*WN*D/SINH(2.0*WN*D))/2.0
   27 FORMAT(E9.2,E10.2,F9.2,9E11.3)
      WRITE(3,27)H,PM,C,T,SSO,DF,DBL,DPB,DT,ATC,CG,CP
 3000 CONTINUE
 1000 CONTINUE
 2000 CONTINUE
      CALL EXIT
      STOP
      END
```

```
C PROGRAM TO CALCULATE FLUID AND BED STREAMFUNCTION VALUES AT VARIOUS
C DEPTHS AND PHASES
C D=DEPTH OF WATER,H=DEPTH OF BED,V=KINEMATIC VISCOSITY,A=AMP,WL=WAVE-
C LENGTH, PM=PERMEABILITY,APM=BOUNDARY CONDITION PARAMETER,SFW=STREAM-
C FUNCTION FOR FLUID,SFB=STREAMFUNCTION IN BED
      DIMENSION SFW(20),SFB(20),SFBL(20)
      PI=3.141592
      G=980.0
      V=0.01
      D=1300.0
      WL=10000.0
      H=700.0
      PM=0.000001
      APM=100.0
      A=100.0
      N=130
      M=8
      Q=M*1.0
      WN=2*PI/WL
      T=SQRT(2.0*PI*WL/(G*TANH(WN*D)))
      F=2*PI/T
      B=SQRT(F/(2*V))
      SD=SINH(WN*D)
      CH=COSH(WN*H)
      ARG2=ATAN(1.0/(APM/B+1.0))
    1 FORMAT(/,3X,'STREAMFUNCTION--WATER')
      WRITE(3,1)
    2 FORMAT(/,3X,'Z=',10X,'0',8X,'22.5',8X,'45',8X,'67.5',8X,'90',7X,'1
     212.5',7X,'135',7X,'157.5',7X,'180 DEGREES')
      WRITE(3,2)
C N=#USED TO PARTITION DEPTH,M=# USED TO PARTITION WAVELENGTH
C DO LOOP FOR DEPTH
      N1=N+1
      DO 1000 K1=1,N1
      K=K1-1
      Z=D-K*D/N
C DO LOOP FOR PHASES AND SFW
      M1=M+1
      DO 800 L=1,M1
      R=L-1.0
      ARG1=PI*R/Q
C SINCE THE BOUNDARY LAYER IS THINNER THAN D/N, NEED TO INCLUDE ITS
C EFFECTS AT Z=0 ONLY
      IF(Z.GT.0) GO TO 90
      C=SQRT(1.0+2.0*B/APM+2.0*(B/APM)**2)
      SFBL(L)=A*F*COS(ARG1+B*Z+ARG2+PI/4.0)/(SD*C*B*1.4)
      SFW(L)=-A*F/SD*(SINH(WN*Z)*COS(ARG1)/WN-COSH(WN*Z)*COS(ARG1+PI/4)/
     2(B*SQRT(2+4*B/APM+(2*B/APM)**2)))+SFBL(L)
      GO TO 800
```

```
   90 SFW(L)=-A*F/SD*(SINH(WN*Z)*COS(ARG1)/WN-COSH(WN*Z)*COS(ARG1+PI/4)/
      2(B*SQRT(2+4*B/APM+(2*B/APM)**2)))
  800 CONTINUE
  801 FORMAT(F8.2,9E11.2)
      WRITE(3,801) Z,(SFW(L),L=1,M1)
 1000 CONTINUE
C NOW FOR SFB
   10 FORMAT(/,3X,'STREAMFUNCTION--BED',/)
      WRITE(3,10)
C DO LOOP FOR BED DEPTH
C NB=# OF VALUES OF Z IN THE BED
      NB=70
      NB1=NB+1
      DO 2000 K1=1,NB1
      K=K1-1
      Z=-K*H/NB
C DO LOOP FOR PHASES AND SFB
      DO 1800 LL=1,M1
      R2=LL-1.0
      ARG4=PI*R2/Q
      SFB(LL)=-A*F*F*PM*SINH(WN*(Z+H))*SIN(ARG4)/(WN*V*SD*CH)
 1800 CONTINUE
 1801 FORMAT(F8.2,9E11.3)
      WRITE(3,1801) Z,(SFB(LL),LL=1,M1)
 2000 CONTINUE
      CALL EXIT
      STOP
      END
```

Appendix 7.4

<u>List of Symbols</u>

a	amplitude
A_1, A_1', A_2	constants
b	boundary layer parameter
*bl	subscript denoting boundary layer
B_1, B_2	constants
c	constant
C	phase speed
C'	constant
C_f	friction coefficient
C_g	group velocity
d	depth of water
d_o	fluid excursion length
D^o	grain diameter
D', D_2	constants
D_{bl}	boundary layer dissipation
D_f	potential flow dissipation
D_{pb}	porous bed dissipation
e	constant = 2.718 $\cdots$
E	energy
f	Fourier sine transform
g	acceleration of gravity
G	function
h	bed depth, gap thickness
H	wave height
i	$\sqrt{-1}$, subscript denoting impermeable bed or initial condition
I	constant
J	constant

k	wave number
k'	von Karman's constant
K	permeability
K_z	eddy viscosity
L	wavelength
n	constant
$*o$	subscript denoting the bottom
p, p_s	pressure
Q_1	seepage velocity, horizontal
Q_2	seepage velocity, vertical
Q, Q_i	horizontal discharge
r	Fourier transform parameter
Re	Reynold's number
Re_c	critical Reynold's number
$*s$	subscript denoting sediment
t	time
T	period
$\underline{u}, \underline{\tilde{u}}_s$	velocity vector
$u', u'_s, \tilde{u}_s, U$	horizontal velocity components
u_b^*	friction velocity
U_0	max horizontal potential velocity at bottom
$w', \tilde{w}_s, w'_s, W$	vertical velocity components
x	horizontal coordinate
z	vertical coordinate
z_0	roughness length

α	boundary condition parameter
β	constant
γ	attenuation coefficient
Γ	circulation
δ	boundary layer thickness
ε	porosity
$\hat{\varepsilon}$	expansion parameter
ζ	parameter
η	surface displacement
Θ	porous bed boundary layer parameter
Θ^*, Θ^-	angle
λ	constant
μ	dynamic viscosity
ν	kinematic viscosity
ξ	constant
π, Π	constant $= 3.14 \cdots$
ρ, ρ_s	density
σ	frequency
ϕ, ϕ_s	velocity potential
Φ, Φ_c	fractional increase in discharge
χ	phase angle
$\psi, \psi^-, \tilde{\psi}_s, \psi_s^-$	stream functions
Ψ	angle
Ω	constant